

Smoke Movement in a Corridor - Hybrid Model,
Simple Model and Comparison with Experiments

Takayuki Matsushita
John H. Klote

Smoke Movement in a Corridor - Hybrid Model, Simple Model and Comparison with Experiments

Takayuki Matsushita
John H. Klote

Building and Fire Research Laboratory
Gaithersburg, MD 20899

December 1992



U.S. Department of Commerce
Barbara Hackman Franklin, *Secretary*
Technology **Administration**
Robert M. White, *Under Secretary for Technology*
National Institute of Standards and Technology
John W. Lyons, *Director*

..
:

·
·
·

List of Tables

| | Page |
|---|------|
| Table 1. Conditions of Experiment (Full Scale) | 14 |
| Table 2. Comparison Between Experiment and Simple Calculation by Zone Model for Time of Overflow on Soffit | 15 |
| Table 3. Sensivity of Froude Number | 16 |
| Table 4. Thermal Sensivity | 17 |
| Table 5. Conditions of Experiment (Reduced Scale Model) | 17 |

List of Figures

| | Page |
|--|------|
| Figure 1. Hybrid Model | 18 |
| Figure 2. A Corridor of Full Scale Experiment | 18 |
| Figure 3. Location of Thermocouple | 19 |
| Figure 4. Smoke Generator | 19 |
| Figure 5. Location of Smoke Front Nose | 20 |
| Figure 6. Distrobution of Horizontal Maximum Temperature | 23 |
| Figure 7. Vertical Temperature Distrobution | 26 |
| Figure 8. Vertical Distrobution of Temperature In Case of Soffit | 31 |
| Figure 9. A Corridor of Reduced Scale Model | 34 |
| Figure 10. Location of Smoke Front Nose (12/100 Scale) | 35 |
| Figure 11. Location of Smoke Front Nose .Comparison Between Full Scale and 12/100 Scale | 35 |
| Figure 12. Location of Smoke Front Nose .Comparison Between Experiment and Calculation | 37 |
| Figure 13. Comparison Between Experiment and Calculation for Location of Front (Nose) after Smoke Inflow (Exp. 1-a) | 40 |
| Figure 14. Comparison Between Experiment and Calculation for Location of Front (Nose) after Smoke Inflow (Exp. 2-a) | 41 |

Smoke Movement in a Corridor - Hybrid Model, Simple Model and Comparison with Experiments

Takayuki Matsushita
John H. Klotz

Abstract

A hybrid model for simulating smoke movement in a corridor is described. This model uses a two zone approach which considers velocities in each zone, and uses a fine mesh in the direction of propagation. Two different approaches to deal with the pressure term are addressed. Full scale and reduced scale experiments are described and compared with the results of the hybrid model. Since heat transfer is not presently incorporated in the hybrid model, the simulated velocity of spread is constant. But in the experiment, the velocity drops with advancing time. A simple model with heat transfer is also described. This model is similar to the density flow model, and assumes that the movement of the smoke front (nose) is similar to the flow through vertical openings in a zone model. Results of the simple model are compared with the experiment with heat transfer, and the effect of the heat transfer coefficient is observed.

Nomenclature

| | |
|-------------|---|
| B | width of corridor m |
| C_p | constant-pressure specific heat kJ/kgK |
| g | gravitational acceleration m^2/s |
| h | height of interface or depth of layer m |
| H | height of ceiling m |
| L | length m |
| P | pressure N/m^2 |
| q | heat transfer rate kJ/m^2s |
| Q | flow rate of smoke m^3/s |
| t | time s |
| T | temperature K |
| V | volume of smoke layer or zone m^3 |
| α | heat transfer coefficient for combined convection and radiation kW/m^2K |
| X | thermal conductivity of wall or ceiling kW/mK |
| ρ | density kg/m^3 |
| ν_{num} | numerical viscosity |

..
:

·
·
·

1. Introduction

To simulate smoke movement in a building fire, it is important to construct a model of the spread of smoke front (nose) in the corridor. Benjamin [1] has developed a treatment of spread of density flow, and Zukoski [2,3] has studied smoke spread by using salt water experiments. These are treatments of the density **flow**, therefore they have ignored the time dependence of density. Heskestad [4] has performed full scale experiments in a corridor by using a burning room, but the boundary condition of the inflow rate in the corridor is uncertain for analyzing the transient smoke spread. Jones and Quintiere [5] have developed an analysis to treat the filling smoke in a corridor by two zone model. But their approach does not model the transient problem before the smoke front arrives at the far wall.

This paper describes a hybrid model of corridor smoke flow without heat transfer, a simple corridor smoke flow model with heat transfer, and corridor smoke flow experiments. Also, experimental data is compared with the predictions of both models. This effort consists of the following parts.

First, the hybrid model is developed. This model is a new approach for considering a transient smoke flow in a corridor, and this method is intermediate between a zone model and a field model. The hybrid model considers the velocity inside each zone to be finite. For simplicity the development of the hybrid model does not presently incorporate the effect of heat transfer. The effect of pressure is dealt with by ignoring the pressure term and also by eliminating the pressure term. These two approaches are referred to in this paper as the *ignored case* and the *eliminated case*.

Second, experiments were conducted with heat loss in a corridor using both a full scale and a small scale model to study the inflow boundary condition and the effect of heat transfer. The similarity between full scale and reduced scale using these experiments is discussed. The Froude number for the flow similarity and the thermal similarity for the effect of heat transfer are addressed. The effect of a soffit, which is a smoke barrier on corridor ceiling, is examined by full scale experiment.

Third, to analyze the effect of heat transfer, a simple model is described based on a macroscopic balance of mass and energy in the smoke flow.

2. Description of Hybrid Model

In this report, the concept of a hybrid model is very restricted. Two dimensionality, no heat transfer, no wall friction and no internal mixing between streams are assumed. These limitations are imposed to simplify the development of the corridor smoke flow model.

2.1 Basic Equations

The hybrid model uses two zones, an upper hot layer (called 'smoke layer') and a lower cold layer (called 'air layer'), for the vertical direction, but uses a fine mesh for the flow horizontal direction. The major difference between the hybrid model and a "normal" zone fire model is how the upper layer is formed. The hybrid model assumes that the layer jet has a finite velocity while the zone model assumes the layer forms instantly.

When mass, momentum and energy equations are integrated for horizontal y-direction and vertical z-

direction of each zone at any x-point, the conservation equation can be written as follows:
Mass Conservation:

$$\int_{0}^{h_2} \int \frac{\partial \rho}{\partial t} dA + \int_{0}^{h_2} \int \frac{\partial \rho u}{\partial x} dA + \int_{0}^{h_2} \int \frac{\partial \rho v}{\partial y} dA + \int_{0}^{h_2} \int \frac{\partial \rho w}{\partial z} dA = 0 \quad (1)$$

Momentum Conservation:

$$\begin{aligned} \int_{0}^{h_2} \int \frac{\partial \rho u}{\partial t} dA + \int_{0}^{h_2} \int \frac{\partial \rho u^2}{\partial x} dA + \int_{0}^{h_2} \int \frac{\partial \rho uv}{\partial y} dA + \int_{0}^{h_2} \int \frac{\partial \rho uw}{\partial z} dA \\ + \int_{0}^{h_2} \int \frac{\partial P}{\partial x} dA + \int_{0}^{h_2} \int \nabla \cdot \tau dA = 0 \end{aligned} \quad (2)$$

Energy Conservation:

$$\begin{aligned} \int_{0}^{h_2} \int \frac{\partial \rho C_p T}{\partial t} dA + \int_{0}^{h_2} \int \frac{\partial \rho C_p Tu}{\partial x} dA + \int_{0}^{h_2} \int \frac{\partial \rho C_p Tv}{\partial y} dA + \int_{0}^{h_2} \int \frac{\partial \rho C_p Tw}{\partial z} dA \\ + \int_{0}^{h_2} \int \frac{\partial q_x}{\partial x} dA + \int_{0}^{h_2} \int \frac{\partial q_y}{\partial y} dA + \int_{0}^{h_2} \int \frac{\partial q_z}{\partial z} dA + \int_{0}^{h_2} \int \tau : \nabla u dA - \int_{0}^{h_2} \int \frac{DP}{Dt} dA = 0 \end{aligned} \quad (3)$$

The equation of state is

$$P = \rho RT \quad (4)$$

where $h_1=0$, $h_2=h$, $\rho=\rho_a$, $u=u_a$, $v=v_a$, $w=w_a$ for the lower cold Layer, and $h_1=h$, $h_2=H$, $\rho=\rho_s$, $u=u_s$, $v=v_s$, $w=w_s$ for the upper hot Layer and h is the height of interface from floor, H the height of ceiling and $dA = dydz$.

2.2 Simplifying Assumptions

For simplicity, the problem is considered as two dimensional (x and z directions only as in Figure 1), and the following assumptions are made:

- a) Constant velocity distribution in each zone
- b) Hydraulic pressure distribution in vertical direction, i.e.

- c) No entrainment on boundary

$$\begin{cases} P = P_f - \rho_a g z & \text{for } z < h \\ P = P_f - \rho_a g h - \rho_s g (z - h) & \text{for } z \geq h \\ P = P_0 - \rho_0 g z & \text{for reference} \end{cases} \quad (5)$$

d) Lower Layer temperature is the same as reference temperature

e) Ignore the effect of viscosity

f) If pressure, P , is a coefficient, P is a constant. If P is included in a derivative, this term is considered.

2.3 Some Basic Relations

The relation for vertical velocity of the moving interface is as follows:

$$\begin{aligned} w_s &= \frac{\partial h}{\partial t} + u_s \frac{\partial h}{\partial x} \\ w_a &= \frac{\partial h}{\partial t} + u_a \frac{\partial h}{\partial x} \end{aligned} \quad (6)$$

The relation of derivative is

$$\begin{aligned} \frac{\partial}{\partial t} \int_{a(x,t)}^{b(x,t)} f(x,t) dz &= f(b) \frac{\partial b}{\partial t} - f(a) \frac{\partial a}{\partial t} + \int_{a(x,t)}^{b(x,t)} \frac{\partial f}{\partial t} dz \\ \frac{\partial}{\partial x} \int_{a(x,t)}^{b(x,t)} f(x,t) dz &= f(b) \frac{\partial b}{\partial x} - f(a) \frac{\partial a}{\partial x} + \int_{a(x,t)}^{b(x,t)} \frac{\partial f}{\partial x} dz \\ \int_{a(x,t)}^{b(x,t)} \frac{\partial f(x,y,t)}{\partial y} dz &= \frac{b-a}{B} [f(x,B,t) - f(x,0,t)] \\ \int_{a(x,t)}^{b(x,t)} \frac{\partial f(x,z,t)}{\partial z} dz &= f(x,b,t) - f(x,a,t) \end{aligned} \quad (7)$$

Therefore the pressure term in eq.(2) is changed by eqs.(5) and (7) as follows:

$$\int_{h_1}^{h_2} \frac{\partial P}{\partial x} dz = (H-h) \frac{\partial P_f}{\partial x} - (\rho_a - \rho_s) g (H-h) \frac{\partial h}{\partial x} \quad \text{for hot layer} \quad (8)$$

$$h \frac{\partial P_f}{\partial x} \quad \text{for cold layer} \quad .$$

The relation between the total pressure, P_f , and the relative pressure, p_f , from a reference point, P_0 , is $p_f = P_f - P_0$. Therefore, the derivative of the total pressure is

$$\frac{\partial P_f}{\partial x} = \frac{\partial p_f}{\partial x} \quad .$$

2.4 Formulation for Hybrid Model with No Heat Transfer

2.4.1 Formulation

Using the above assumptions and relations, the following formulation for the case of incompressible flow with no heat transfer to the walls is obtained.

From mass conservation of the hot layer, the equation of change of interface height, h , can be written as follows:

$$\frac{\partial h}{\partial t} + u_s \frac{\partial h}{\partial x} - (H-h) \frac{\partial u_s}{\partial x} = 0 \quad . \quad (9)$$

From mass conservation of hot and cold layers,

$$\frac{\partial (H-h)u_s}{\partial x} + \frac{\partial hu_a}{\partial x} = 0 \quad . \quad (10)$$

Therefore under the boundary condition $h = h_0$ and $u_s = u_{s0}$ at $x = 0$ and the open at the other boundary, the relation of mass conservation on an arbitrary vertical plane is

$$(H - h)u_s + hu_a = (H - h_0)u_{s0} \quad (11)$$

where u_{s0} is the inflow velocity and h_0 is the interface height from the floor at boundary $x=0$.

From momentum and mass conservation of the hot layer, the equation of change of velocity in hot layer is written as follows:

$$\frac{\partial u_s}{\partial t} - \frac{\rho_a - \rho_s}{\rho_s} g \frac{\partial h}{\partial x} + u_s \frac{\partial u_s}{\partial x} + \frac{1}{\rho_s} \frac{\partial P_f}{\partial x} = 0 \quad (12)$$

From momentum and mass conservation of cold layer, the equation of change of velocity in cold layer is as follows:

$$\frac{\partial u_a}{\partial t} + u_a \frac{\partial u_a}{\partial x} + \frac{1}{\rho_a} \frac{\partial P_f}{\partial x} = 0 \quad (13)$$

2.4.2 Eliminating the Pressure Term (Eliminated Case)

For the hybrid model with no heat transfer, the system consists of equations (9), (11), (12) and (13) with unknown variables h , u_s , u_a and P_f . These equations can be simplified by using equation (13) to eliminate $\partial P_f / \partial x$ and equation (11) to explicitly determine u_a .

The equation of change of hot layer velocity is modified as follows:

$$C \frac{\partial u_s}{\partial t} + \left[-\frac{\rho_a - \rho_s}{\rho_s} g - (u_a - u_s) DE \right] \frac{\partial h}{\partial x} + \left[u_s + E u_a \frac{H-h}{h} - DE(H-h) \right] \frac{\partial u_s}{\partial x} = 0 \quad (14)$$

where $C = 1 + \frac{\rho_a(H-h)}{\rho_s h}$, $D = -\frac{u_{s0}(H-h)}{h^2} + \frac{H}{h^2} u_s$, $E = \frac{\rho_a}{\rho_s}$

and

$$u_a = \frac{u_{s0}(H-h_0) - (H-h)u_s}{h} \quad (15)$$

This system can then be solved using eqs.(9) and (14) under the boundary condition, $h=h_0$ and $u_s=u_{s0}$ at $x=0$. The term u_a is calculated using explicitly by eq.(15).

2.4.3 Ignoring the Pressure Term (Ignored Case)

The other treatment is to ignore the pressure term by setting $\partial P_f / \partial x$ to zero. When the pressure term in eqs.(12) and (13) is ignored, only eq.(12) is used and eq.(13) is unnecessary.

$$\frac{\partial u_s}{\partial t} - \frac{\rho_a - \rho_s}{\rho_s} g \frac{\partial h}{\partial x} + u_s \frac{\partial u_s}{\partial x} = 0 \quad (16)$$

u_a is the same as the eliminated case, so the relation of eq.(15) can be used. In this case, eqs.(9) and (16) are used to solve under the same boundary condition as the eliminated case.

2.5 Numerical Method

To solve this system of partial differential equations, the subroutine package "**PDECOL**" was used. In this case, the numerical viscosity term, $\nu_{num} \partial^2 u / \partial x^2$, was needed in order to calculate stably in eq.(14) or eq.(16). For the calculations of this paper, a value of ν_{num} of 0.1 resulted in numerical stability.

3. Experiments

3.1 Full Scale Experiment

3.1.1 Facility

Full scale experiments for corridor smoke flow were run at the Building Research Institute (**BRI**) in Japan. Figure 2 shows the plan and the section of experimental corridor underground. The length of the corridor was about 65 m, and the ceiling height was 2 m. The corridor width changes at two locations, and the 40 m long section of corridor with a constant width of 1.5 m was used for these experiments. To study the effects of the soffit to prevent smoke movement, a soffit is located at 23 m of the inlet of smoke.

At every 2 m along the corridor length, eight thermocouples are located vertically **as** shown in Figure 3. The thermocouples were made of 0.32 mm diameter type-T thermocouple wire. The shape of smoke inlet from the one side of the corridor was 0.3 m depth from the ceiling and 1.2 m width, and the other side was open. The location of smoke front was measured by eye.

Figure 4 shows that the smoke generator apparatus was composed of an inlet nozzle, **an** air supply fan, a smoke generator machine and an electric heater (maximum about 30 kW). The power of the air supply fan is variable . The strength of heat source is able to change in 3 stages. The inflow rate of outside air was calculated from measurements of the pressure difference between the inlet nozzle and outside. Triethylene glycol was mixed by the smoke generator machine in the front of heater. Before the inflow of smoke to corridor, the bypass route was **used** until temperature and flow rate in the smoke generator apparatus approached steady state. The damper was set so that the resistance of bypass route **was** nearly the same **as** that of route to corridor inlet. The temperature of inflow to corridor and the inflow rate of air were measured. Therefore, the boundary conditions were known for the analysis of smoke spread in corridor.

3.1.2 Experimental Conditions

Table 1 shows the experimental conditions. In this table, group-1 is the low flow (about 0.24 m³/s) and medium temperature (about 50-56 °C), group-2 is the low flow and high temperature (about 64-70 °C), group-3 is the high flow (about 0.4 m³/s) and low temperature (about 42 °C), group-4 is the high flow and medium temperature and group 5 is the high flow and high temperature for the inflow condition of smoke. The sub group-a means the no soffit case, sub group-b means the 0.5 m height soffit and sub group-c means the 1.0 m depth of soffit.

3.1.3 Experimental Results

The experimental results are shown in figures 5 to 8. Figure 5 is the location of smoke front after smoke inflow for all of the experiments listed in table 1. This figure shows the effect of soffits on smoke movement. The deeper the soffit, the smaller the smoke movement velocity and depth after the soffit and the deeper the smoke layer before the soffit. The comparison of all experiments shows, in general, that the smoke spread is faster for high flow and for high temperature. Thus, the effect of heat transfer is important.

Figure 6 shows the horizontal distribution of smoke temperature for all of the full scale experiments. This shows the location of smoke front by the measurement of temperature. The maximum temperature decreases with distance from the inlet of smoke.

Figure 7 shows the vertical temperature distribution for each horizontal location from smoke inlet in the experiment No.5-a. At each horizontal location, the temperature in smoke zone and the ceiling temperature is nearly constant.

Figure 8 shows the temperature change of before and after the soffit in the experiment group-2. This shows that temperature and smoke layer depth decrease after a soffit and the depth of smoke increases before a soffit.

Table 2 shows the comparison between the simplest two zone model with no entrainment and the experimental results for the overflow time on the soffit. The overflow time in experiments is faster than the simple prediction. For reference, the arrival time at 40 m from the smoke inlet for the experiment is shown.

3.2 Reduced Scale Model

3.2.1 Similarity of Flow

This section discusses the similarity between full scale and scaled model for a corridor smoke flow. First the flow is dominated by the Froude number:

$$Fr = \frac{u}{\left(\frac{\rho_a - \rho_s}{\rho_s} g L\right)^{1/2}} \quad (17)$$

The density and gravity are considered the same in a full scale and a small scale model. As the reduced scale is determined by our purpose, velocity is affected. Now the suffix "full" means full scale and suffix "model" means small scale model. Then the ratio of velocity is

$$u_{model}/u_{full}=(L_{model}/L_{full})^{1/2} \quad (18)$$

The flow rate can be described by $L*u$. Therefore, the inflow rate ratio is

$$Q_{model}/Q_{full}=(L_{model}/L_{full})^{5/2} \quad (19)$$

Time is described by L/V , therefore

$$t_{model}/t_{full}=(L_{model}/L_{full})^{1/2} \quad (20)$$

Now in our reduced scale model, $L_{model}/L_{full}=12/100$. The relation of these properties is shown in Table 3.

3.2.2 Similarity of Thermal Effect

Considering an averaged temperature in the hot layer, semi infinite walls (and ceilings), and constant wall temperature; thermal similarity for wall is [6]

$$(\lambda\rho C_p)_{model}/(\lambda\rho C_p)_{full}=(L_{model}/L_{full})^{3/2} \quad (21)$$

The walls and ceiling are made from concrete in full scale and from Acrylic Plate in small scale model. These properties are shown in Table 4, and this table also shows that the similarity of thermal effects between full scale and small scale is good.

Table 5 shows the experimental condition corresponding to high flow experiment of full scale.

3.2.3 Apparatus

Figure 9 shows the plan and the section of the reduced scale model. Acrylic Plate was chosen for the model so that the location of smoke front could be observed.

The smoke generator machine is similar as a full scale experiment, but the inflow rate is reduced. The scale of this model is **121100**. The height and the width of corridor are similar to a full scale corridor, and the inflow shape is also the same. The location of smoke front is observed from video recordings.

3.2.4 Comparison of Full Scale and Reduced Scale Model

Figure 10 shows the results of the location of smoke front in all reduced scale model experiments. This shows the same feature as full scale experiments.

Figure 11 shows the comparison for the location of smoke front between a full scale and a small scale model experiment for the corresponding condition. As the time scale and the length scale are for a full

scale, the result of reduced scale model is corrected. There is good agreement between the small scale experiments and the full scale experiments.

4. Comparison Between Hybrid Model and Experiment

4.1 Comparison between Experiments and Calculation Results

Figure 12 shows the location of smoke front from the experiments and from simulations of the hybrid model for both the eliminated case and the ignored case. The 40 m corridor was divided into 200 cells. For about the first 10 seconds, the hybrid model is in good agreement with the experiments. However, after 10 seconds, the spread speed decreases in the experiment, but it stays constant in the hybrid model. This is because this model assumes constant density and no heat loss. This spread speed is smaller than the case of Froude number = 1.414 and greater than the case of $Fr = 1$.

4.2 Comparison of Treatments of the term of Pressure

Figures 13 through 17 show the smoke spread from simulations of the hybrid model for both the eliminated case and the ignored case. The smoke front travels faster for the ignored case simulations than it does for the eliminated case simulations. The depth of the smoke layer of the ignored case is less than that of the eliminated case. Thus, the treatment of the pressure term is important.

5. Simple Model With Heat Transfer

5.1 Simple Model

The effect of heat transfer on the movement of the hot layer movement in a corridor is very important. The first step in the treatment of heat loss is a simple zone model at the macroscopic level. Usually zone models assume a uniform density in one zone and the following relation between the velocity and the pressure difference at an opening:

$$\frac{\rho_s u_f^2}{2} = \Delta P \quad . \quad (22)$$

Considering the hydrostatic pressure distribution in the vertical direction in the same manner as is done for zone models, the pressure difference at the front of smoke flow is

$$\Delta P = \Delta \rho g z \quad (23)$$

where $\Delta \rho = \rho_a - \rho_s$.

From eqs.(22) and (23), the equation of hot layer velocity at any height is

$$u_f = \left(\frac{2\Delta \rho g z}{\rho_s} \right)^{1/2} \quad (24)$$

The volumetric flow rate of the nose, Q_f is

$$\begin{aligned} Q_f &= b \int_0^{h_f} u_f dz \\ &= \frac{2}{3} b \left(\frac{2\Delta \rho g}{\rho_s} \right)^{1/2} h_f^{3/2} \end{aligned} \quad (25)$$

As Q_f equals the inflow rate on the boundary at $x=0$, Q_0 , for the constant inflow condition, the depth, h_f , and the averaged velocity, $(u_f)_{mean}$, of hot layer front is obtained.

$$h_f = \left(\frac{3}{2} \right)^{2/3} \left(\frac{2\Delta \rho g}{\rho_s} \right)^{-1/3} \left(\frac{Q_0}{b} \right)^{2/3} \quad (26)$$

$$\begin{aligned} (u_f)_{mean} &= Q_f / (bh_f) \\ &= 2 \cdot 3^{-2/3} \left(\frac{\Delta \rho g Q_0}{\rho_s b} \right)^{1/3} \end{aligned} \quad (27)$$

To deal with heat loss, the following are assumed:

- a) The hot layer temperature is uniform.
- c) The temperature of wall and ceiling is constant.
- b) The heat loss to wall and ceiling is treated by following simple equation

$$q = \alpha(T_s - T_w) \quad (28)$$

For these assumptions, the mass and energy equations for hot layer are developed. The conservation of mass equation for the hot layer is as follows:

$$\frac{d(\rho_s V_s)}{dt} = \rho_0 Q_0 \quad (29)$$

The conservation of energy equation for the hot layer is as follows:

$$(C_p \rho_s V_s) \frac{dT_s}{dt} = C_p \rho_0 Q_0 T_0 - q A_s \quad (30)$$

From eqs.(29) and (30), average temperature change in hot layer in the layer is

$$(C_p \rho_s V_s) \frac{dT_s}{dt} = C_p \rho_0 Q_0 (T_0 - T_s) - A_s \alpha (T_s - T_w) \quad (31)$$

5.2 Comparison between Experiments and Simple Model Results

The system of eqs.(27) and (31) provides the hot layer spread speed and the averaged temperature. For simplicity, eq.(31) can be calculated by the explicit method.

Figure 18 shows the location of smoke front for the experimental results and the calculation results for heat transfer coefficient 0.0 (a case of no heat loss), 17.4 and 23.3 W/m², and for reference the results of the hybrid model. At the early stage of smoke flow (before 20 s), the measured smoke spread is faster than the calculated results of the simple model. However, after about 20 seconds, the agreement is good between experiments and the calculations of the simple model with a heat transfer coefficient of 23.3.

6. Conclusions

The hybrid model for smoke movement in a corridor, without heat transfer to the walls, shows good agreement with experimental data for a 40 m full scale corridor until 10 seconds after smoke inflow. As the spread speed in the hybrid model with no heat transfer is constant, after 10 seconds the agreement is bad because the velocity in the experiments decrease gradually.

The experiments with reduced scale model were in good agreement with full scale experiments by considering the similarities of the flow and the thermal.

The calculations using simple model with heat transfer were in good agreement with the experiment. However, at the beginning of the simulation (for small time values of time), the prediction is smaller than the results of experiment.

A simple model with heat transfer is useful to evaluate the approximate smoke spread in a corridor. Because the heat transfer is an important factor in smoke spread, a hybrid model with heat transfer is needed for more accurate treatment.

7. Acknowledgements

The author would like to thank John H. Klotz of NIST for the management support necessary for the work on the hybrid model. Credit for the idea of the hybrid model should be given to Walter W. Jones and Howard R. Baum of NIST. The author appreciated the chance to develop this concept. And the author appreciates T. Wakamatsu (Tokyo Science University), T. Yamana (**ERI**), H. Nakamura (Shimizu Corporation), and students of Tokyo Science University for the cooperation of the full scale and the small scale experiments.

8. References

- [1] T.B.Benjamin; Gravity Currents and Related Phenomena, J. Fluid Mech., 31, 209-248.
- [2] E.E.Zukoski and T.Kubota; Experimental Study of Environment and Heat Transfer in a Room Fire, NIST-GCR-88-554, Nov. 1988.
- [3] M.V.Chobotov, E.E.Zukoski and T.Kubota; Gravity Currents with Heat Transfer Effects, NBS-GCR-87-522, Dec. 1986.
- [4] G.Heskestad and J.P.Hill; Experimental Fires in Multiroom/ Corridor Enclosures, NBS-GCR-86-502.
- [5] W.W.Jones and J.G.Quintiere; Prediction of Corridor Smoke Filling by Zone Model, Combustion Science and Tech., 1984, 35.
- [6] M.Tsujimoto; A Scaling Law of Smoke Movement in Atrium, 11th UJNR on Fire Research and Safety, 181-187, 1989.

Table 1 Conditions of Experiment(Full Scale)

| EXP. No. | Soffit Height [m] | Inlet Air Rate [m ³ /s] | Inlet Smoke Temp. [°C] | Corridor Temp. [°C] | Outside Temp. [°C] |
|----------|----------------------|---------------------------------------|---------------------------|------------------------|-----------------------|
| 1-a | 0.0 | 0.248 | 48.0 | 23.6 | 28.0 |
| 1-b | 0.5 | 0.257 | 50.1 | 24.3 | 26.5 |
| 1-c | 1.0 | 0.246 | 51.1 | 24.5 | 26.6 |
| 2-a | 0.0 | 0.233 | 64.8 | 23.7 | 28.2 |
| 2-b | 0.5 | 0.238 | 64.9 | 24.3 | 28.0 |
| 2-c | 1.0 | 0.245 | 67.4 | 23.8 | 26.6 |
| 3-a | 0.0 | 0.401 | 43.7 | 24.5 | 28.1 |
| 3-b | 0.5 | 0.402 | 42.7 | 24.3 | 28.1 |
| 3-c | 1.0 | 0.375 | 42.3 | 22.9 | 26.3 |
| 4-a | 0.0 | 0.398 | 56.3 | 23.7 | 30.0 |
| 4-b | 0.5 | 0.383 | 56.1 | 24.1 | 27.5 |
| 4-c | 1.0 | 0.381 | 57.3 | 23.1 | 31.8 |
| 5-a | 0.0 | 0.360 | 68.1 | 22.8 | 28.4 |
| 5-b | 0.5 | 0.393 | 68.5 | 24.1 | 26.6 |
| 5-c | 1.0 | 0.395 | 69.7 | 24.6 | 27.3 |

* Group Condition

Exp. 1=Low Flow Rate & Mid. Temperature
 Exp. 2=Low Flow Rate & High Temperature
 Exp. 3=High Flow Rate & Low Temperature
 Exp. 4=High Flow Rate & Mid. Temperature
 Exp. 5=High Flow Rate & High Temperature

Table 2 Comparison between Experiment and Simple Calculation by Zone Model
for Time of Overflow on Soffit (point of 23m from inlet)

| EXP. No. | Soffit Height [m] | Time of Overflow on Soffit | | Exp. Arrival Time at 40m from inlet [s] |
|----------|----------------------|----------------------------|--------------------------------------|---|
| | | Exp. Result [s] | Cal. by Two <i>bre</i> Model. [s] | |
| | 0.0 | 39 | -- | 121 |
| | 0.5 | 54 | 67 | 127 |
| | 1.0 | 57 | 139 | 139 |
| 2-a | 0.0 | 39 | -- | 108 |
| 2-b | 0.5 | 42 | 72 | 118 |
| 2-c | 1.0 | 46 | 140 | 124 |
| 3-a | 0.0 | 46 | -- | 100 |
| 3-b | 0.5 | 45 | 43 | 114 |
| 3-c | 1.0 | 51 | 92 | 123 |
| 4-a | 0.0 | 38 | -- | 89 |
| 4-b | 0.5 | 36 | 45 | 96 |
| 4-c | 1.0 | 36 | 91 | 107 |
| 5-a | 0.0 | 30 | -- | 79 |
| 5-b | 0.5 | 34 | 43 | 84 |
| 5-c | 1.0 | 42 | 87 | 102 |

*Use of Two Zone Model without Entrainment

Table 3 Similarity of Froude Number

$$Fr_m = Fr_f : Fr = V / ((\Delta\rho/\rho) \cdot g \cdot L)^{1/2}$$

| | Full Scale | Small Scale | Condition or Similarity |
|-------------|------------|-------------|--|
| Temperature | T_f | T_m | $T_m = T_f \rightarrow$ Thermal Similarity |
| Density | ρ_f | ρ_m | $\rho_m = \rho_f$ |
| gravity | g_f | g_m | $g_m = g_f$ |
| Scale | L_f | L_m | $L_m/L_f = 1/2$ |
| Velocity | V_f | V_m | $V_m/V_f = (L_m/L_f)^{1/2} = 0.346$ |
| Inflow Rate | Q_f | Q_m | $Q_m/Q_f = (L_m/L_f)^{5/2} = 0.00499$ |
| Time | t_f | t_m | $t_m/t_f = (L_m/L_f)^{1/2} = 0.346$ |

Table 4 Thermal Similarity

$$(\lambda \rho C_p)_m / L_m^{3/2} = (\lambda \rho C_p)_f / L_f^{3/2}$$

| | | | Full Scale (Concrete) | Small Scale (Acrylic) |
|---|--------------------------------------|-----------|--------------------------|--------------------------|
| Density | [Kg/m ³] | ρ | 2.4×10^3 | 1.19×10^{-3} |
| Specific Heat | [kJ/kgK] | C_p | 0.84 | 1.465 |
| Thermal Conductivity | [kW/mK] | λ | 1.0×10^{-2} | 2.09×10^{-4} |
| Thermal Diffusivity | $\frac{[\text{ch}]}{A} / (\rho C_p)$ | | 4.96×10^{-6} | 1.20×10^{-7} |
| $\lambda \rho C_p$ | | | 2.02×10 | 3.64×10^{-1} |
| Thermal Similarity | | | 20.2 | 8.75 |
| $(\lambda \rho C_p) / L^{3/2} : L_m / L_f = 12 / 100$ | | | | |

Table 5 Conditions of Experiment (Reduced Scale Model)

| EXP. No. | Inlet Smoke Rate [m ³ /s] | Inlet Smoke Temp. [°C] |
|----------|---|---------------------------|
| 3-m | 0.002 | 44 |
| 4-m | 0.002 | 56 |
| 5-m | 0.002 | 77 |

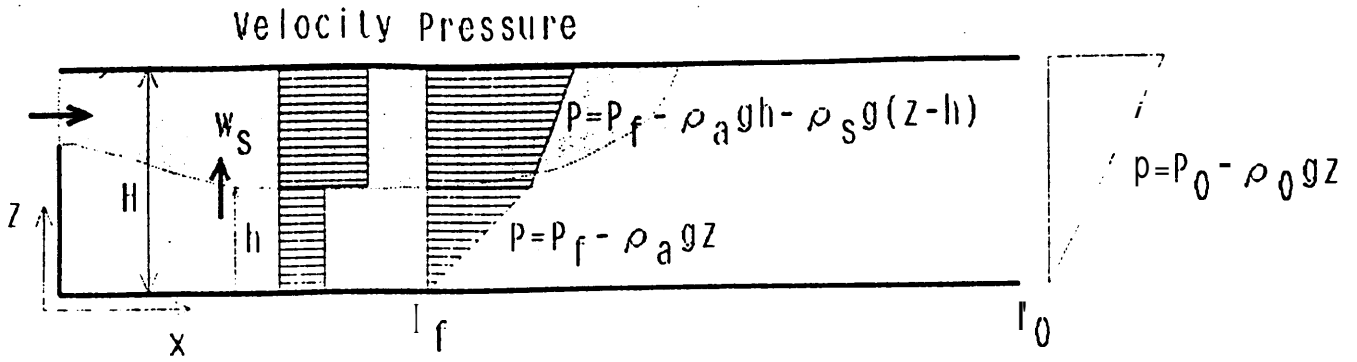
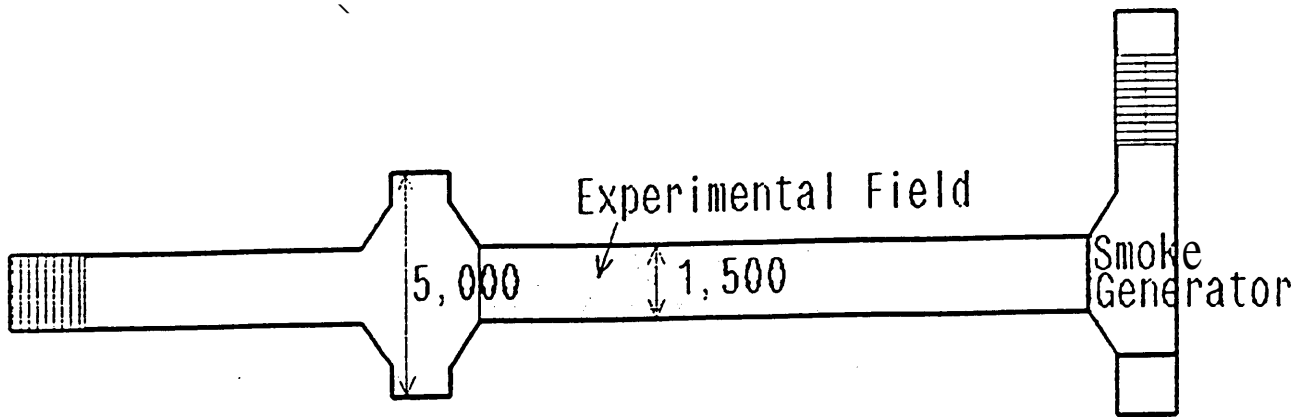
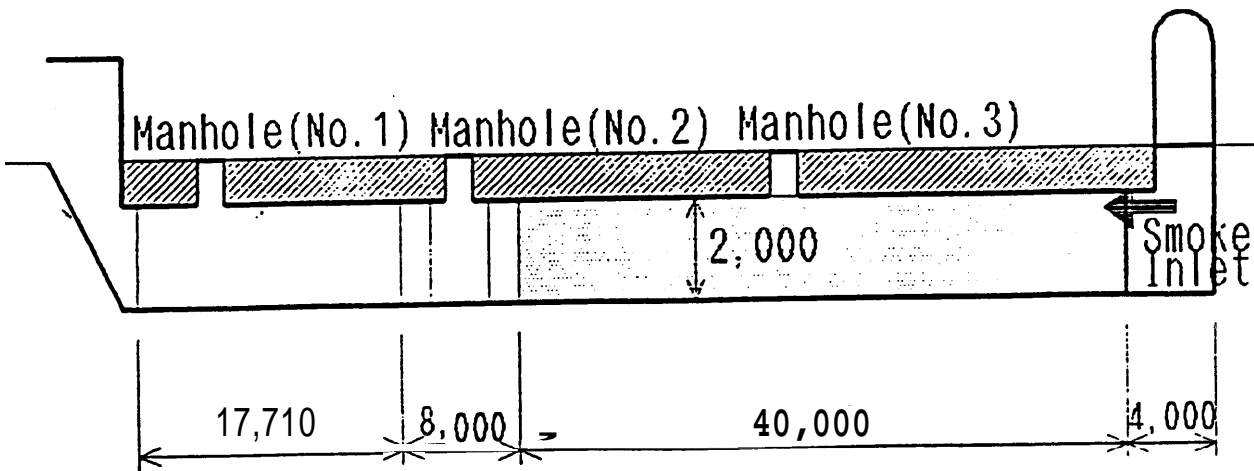


Figure 1 Hybrid Model



Corridor Plan



Corridor Section

BRI Under-ground Corridor

Figure 2 A Corridor of Full Scale Experiment

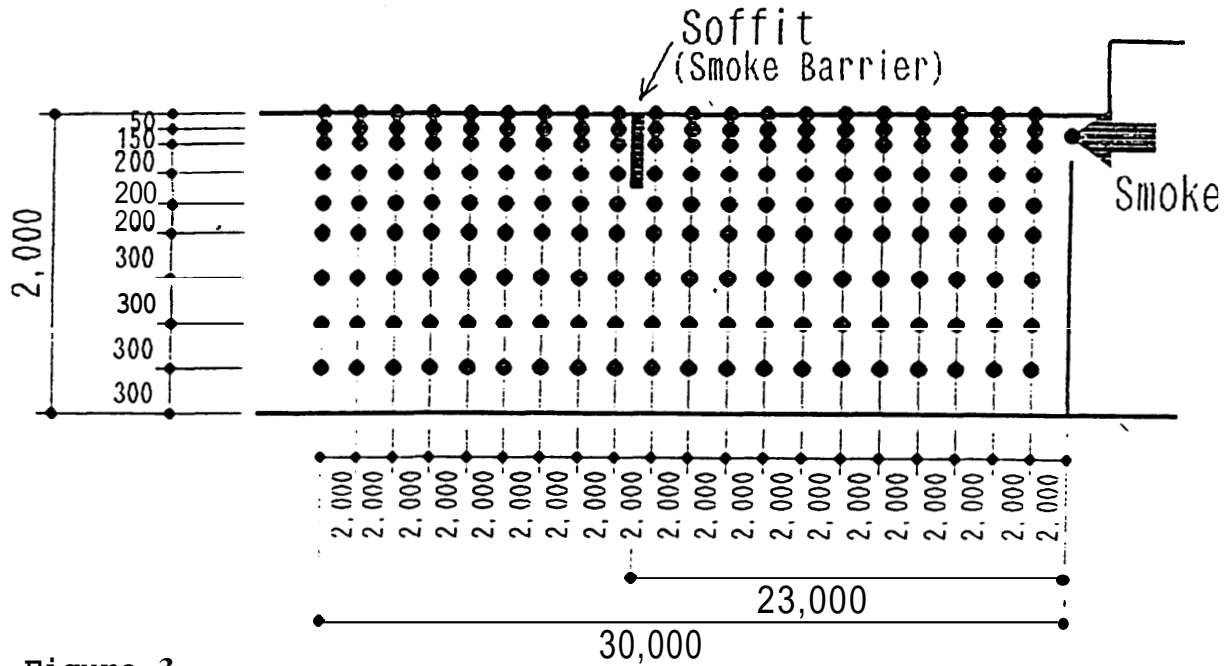


Figure 3

Location of Thermo Couple (Type-T:0.32mm ϕ)

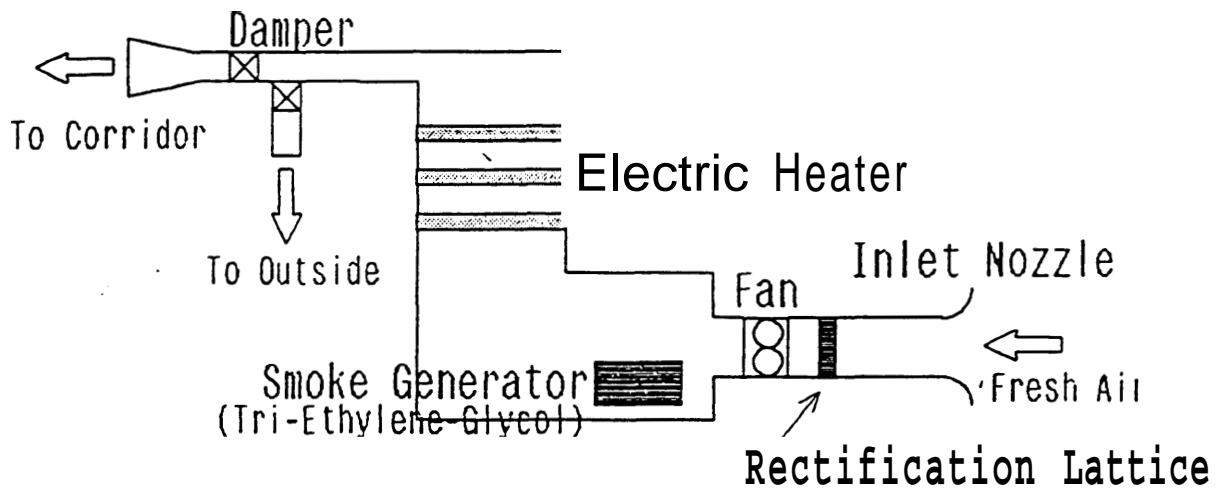


Figure 4

Smoke Generator

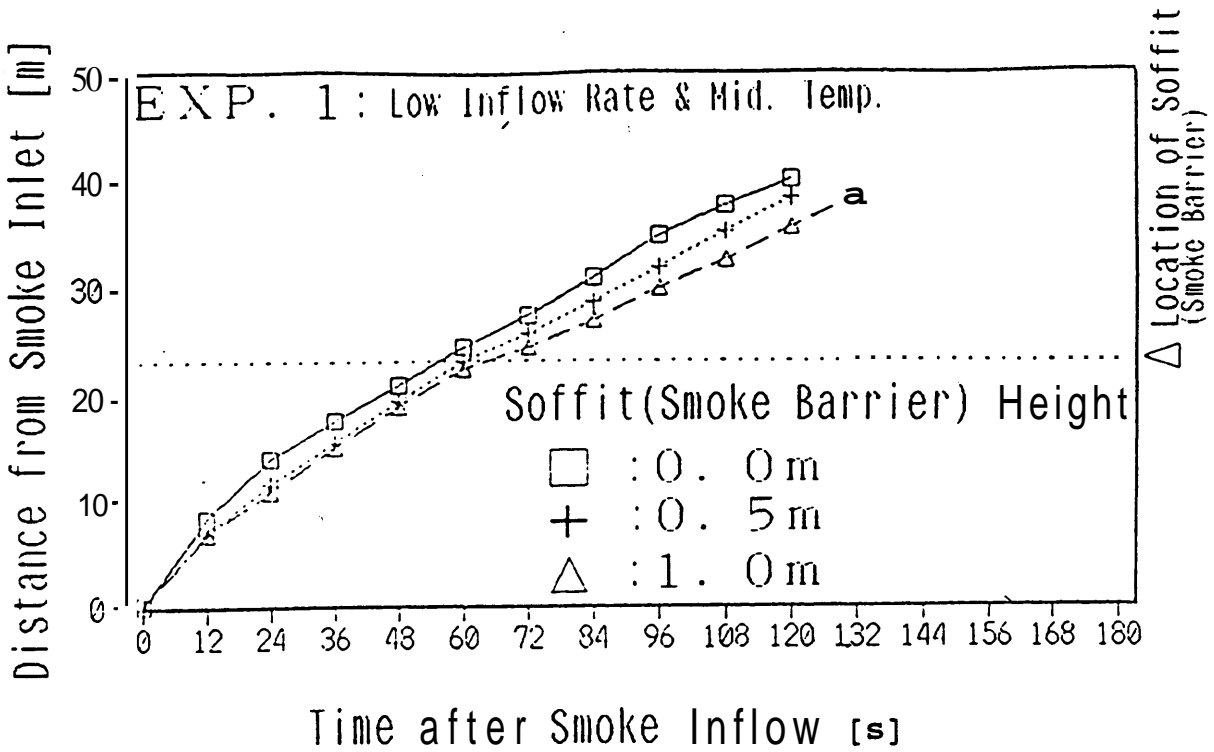


Figure 5-a Location of Smoke Front Nose (Exp.1)

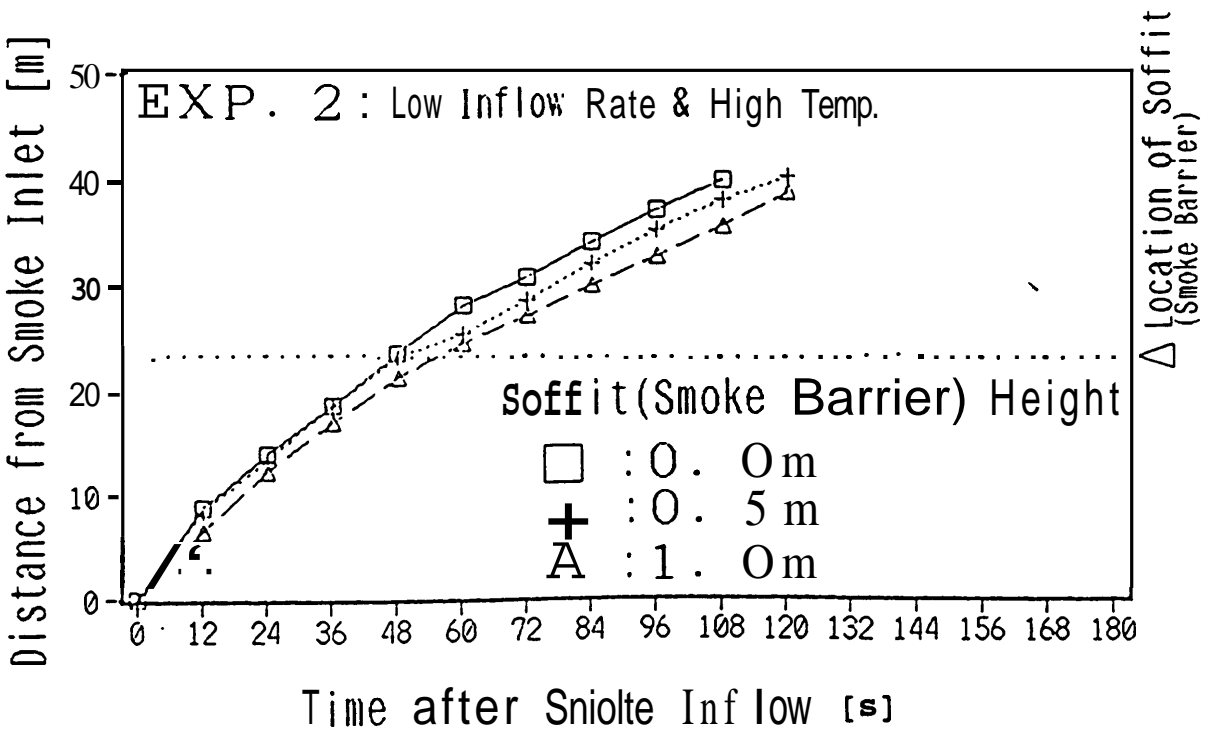


Figure 5-b Location of Smoke Front Nose (Exp.2)

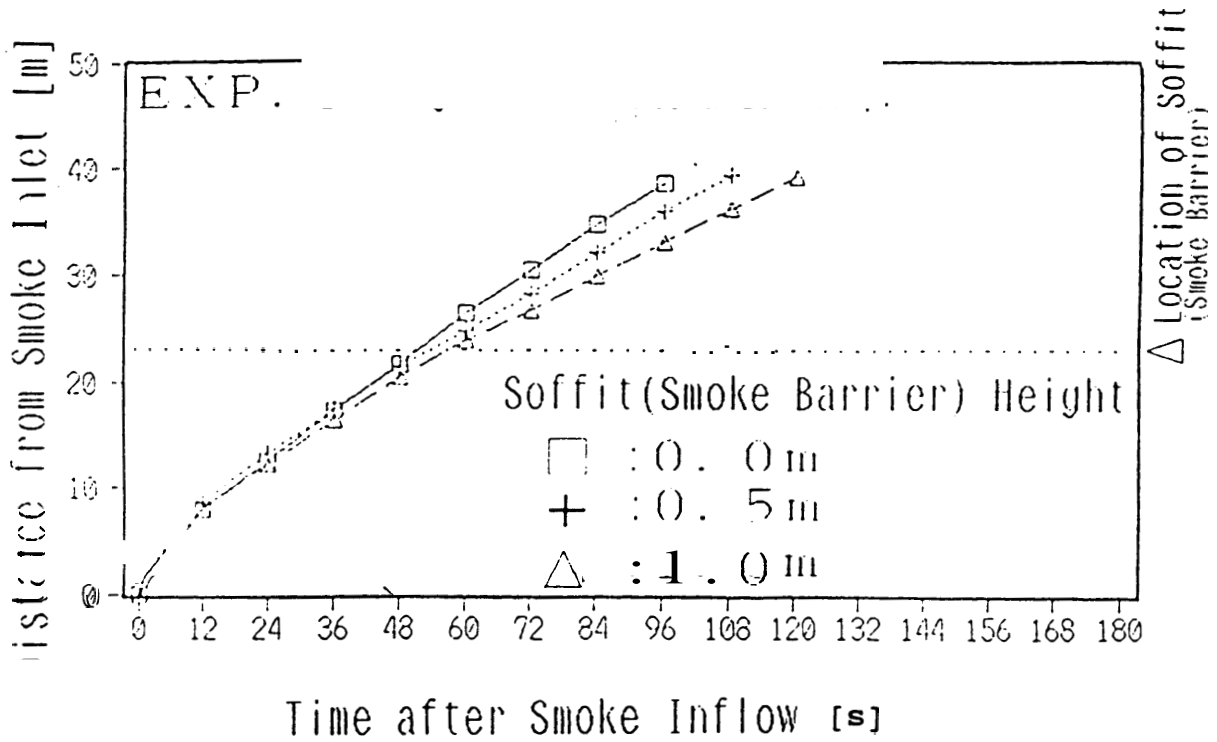


Figure 5-c Location of Smoke Front Nose (Exp.3)

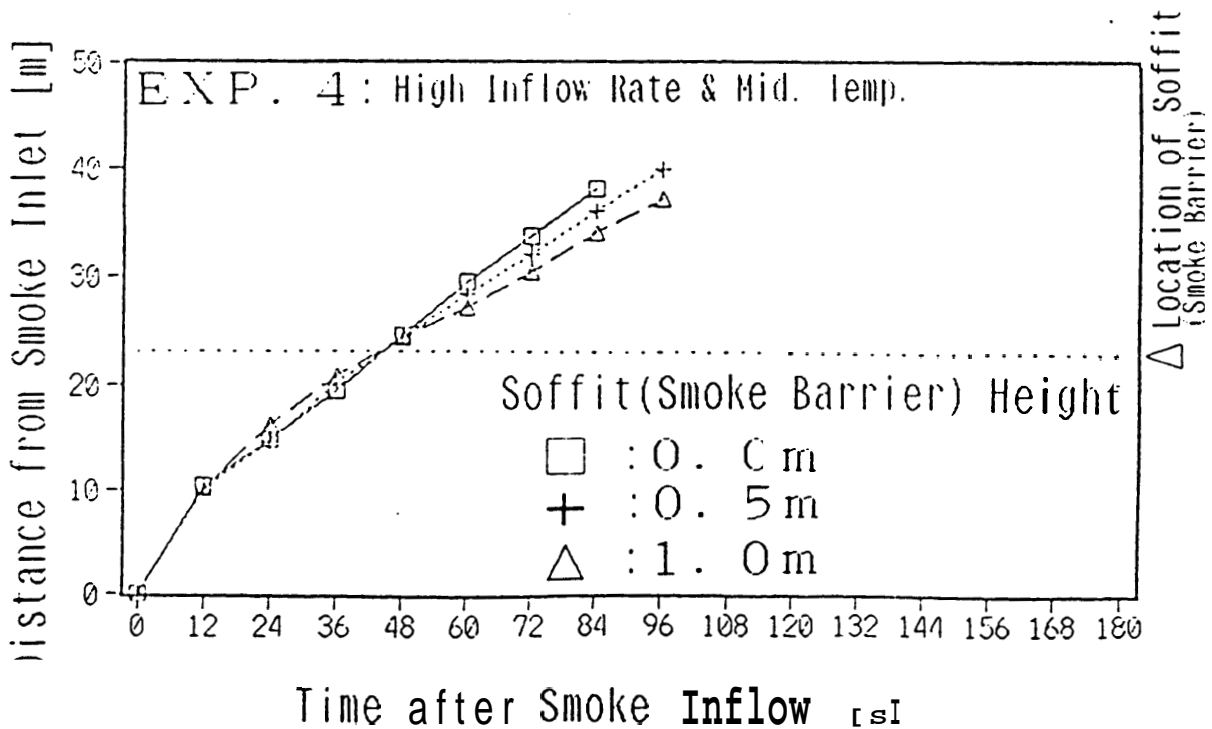


Figure 5-d Location of Smoke Front Nose (Exp.4)

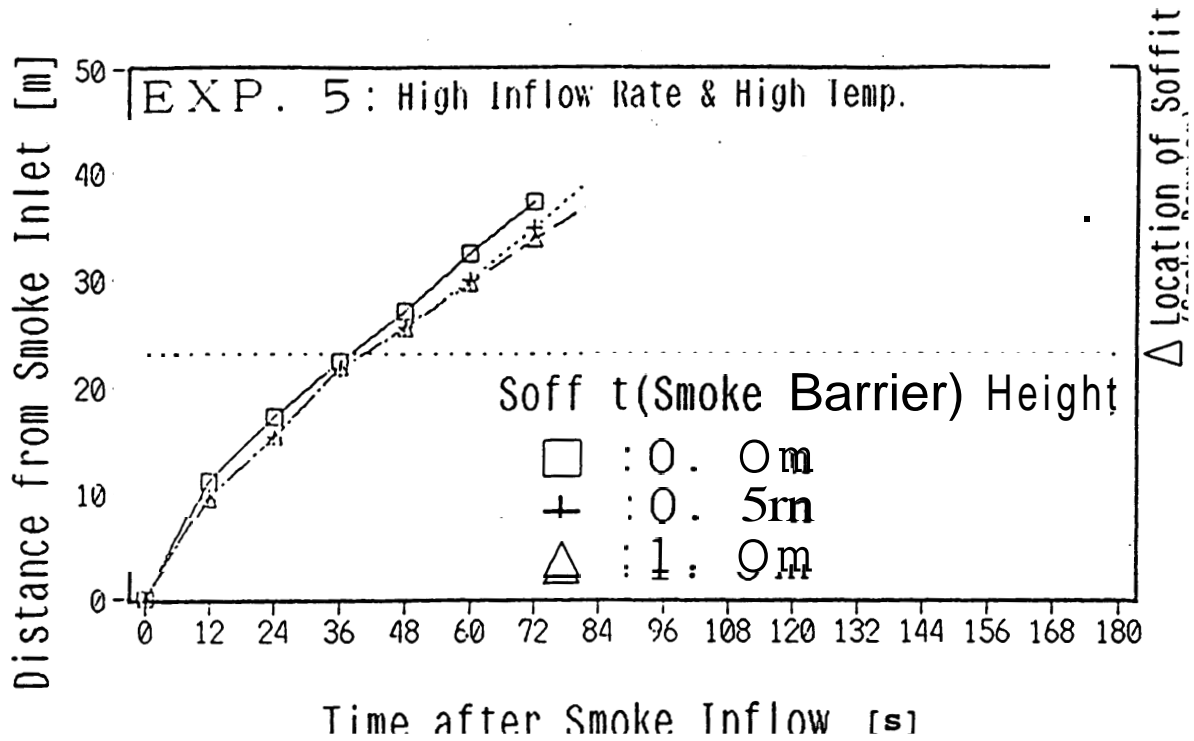


Figure 5-e Location of Smoke Front Nose (Exp. 5)

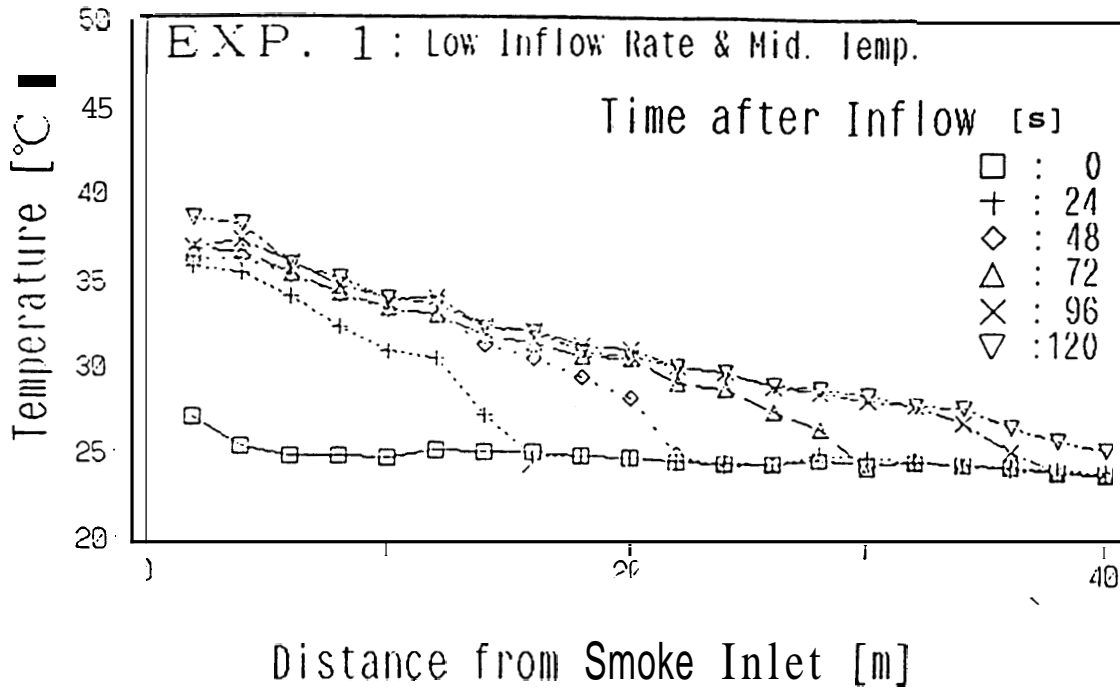


Figure 6-a Distribution of Horizontal Maximum Temperature (Exp.1-a)

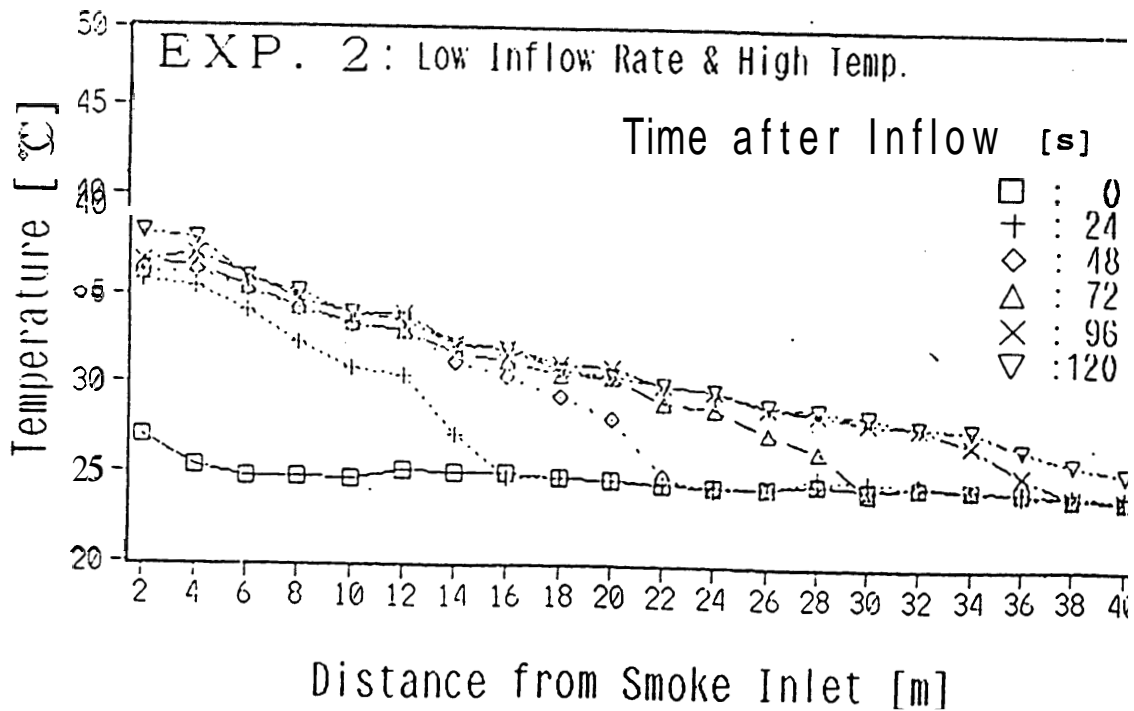


Figure 6-b Distribution of Horizontal Maximum Temperature (Exp.2-a)

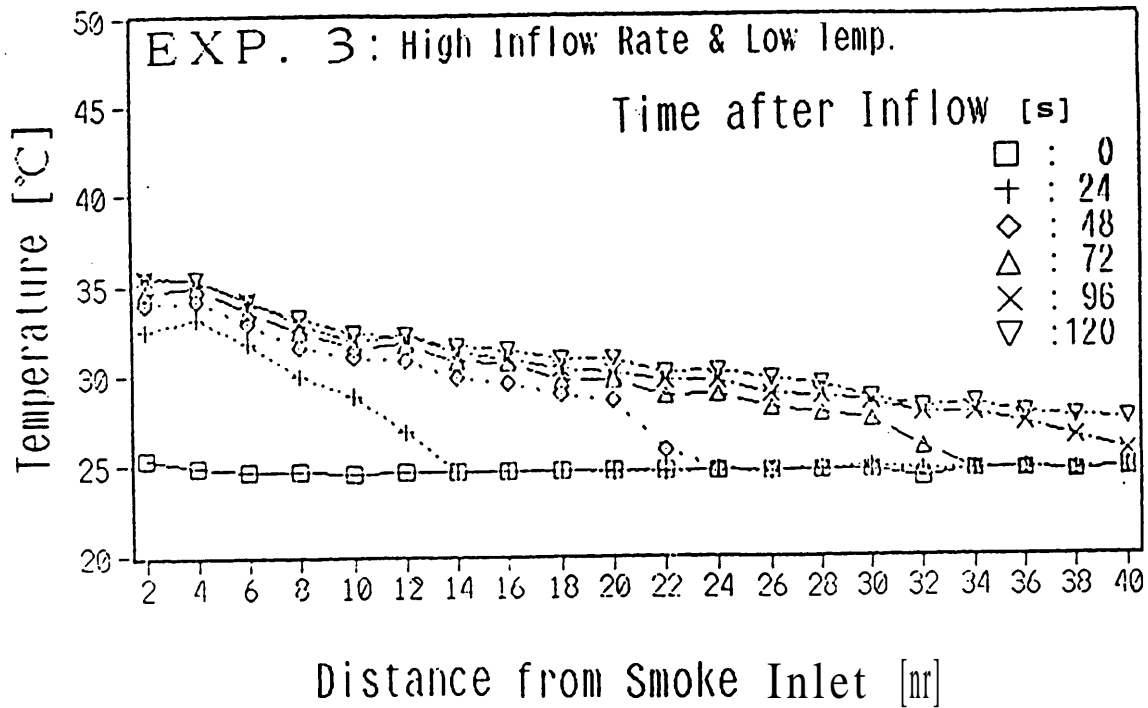


Figure 6-c Distribution of Horizontal Maximum Temperature (Exp. 3-a)

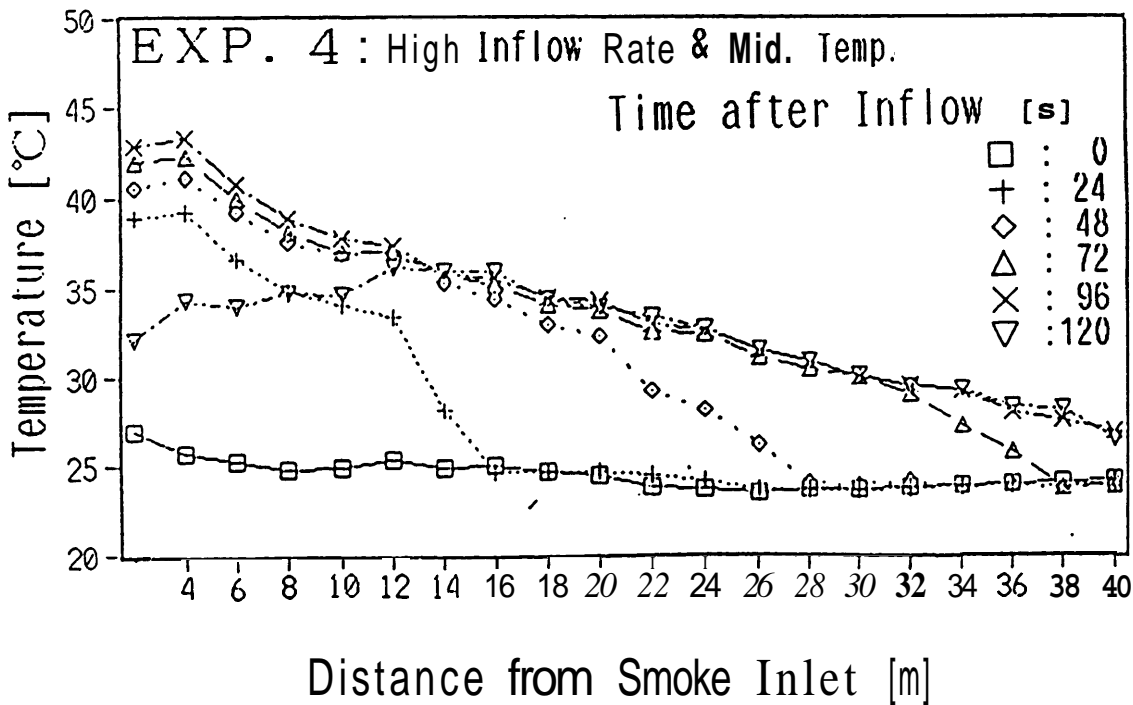


Figure 6-d Distribution of Horizontal Maximum Temperature (Exp. 4-a)

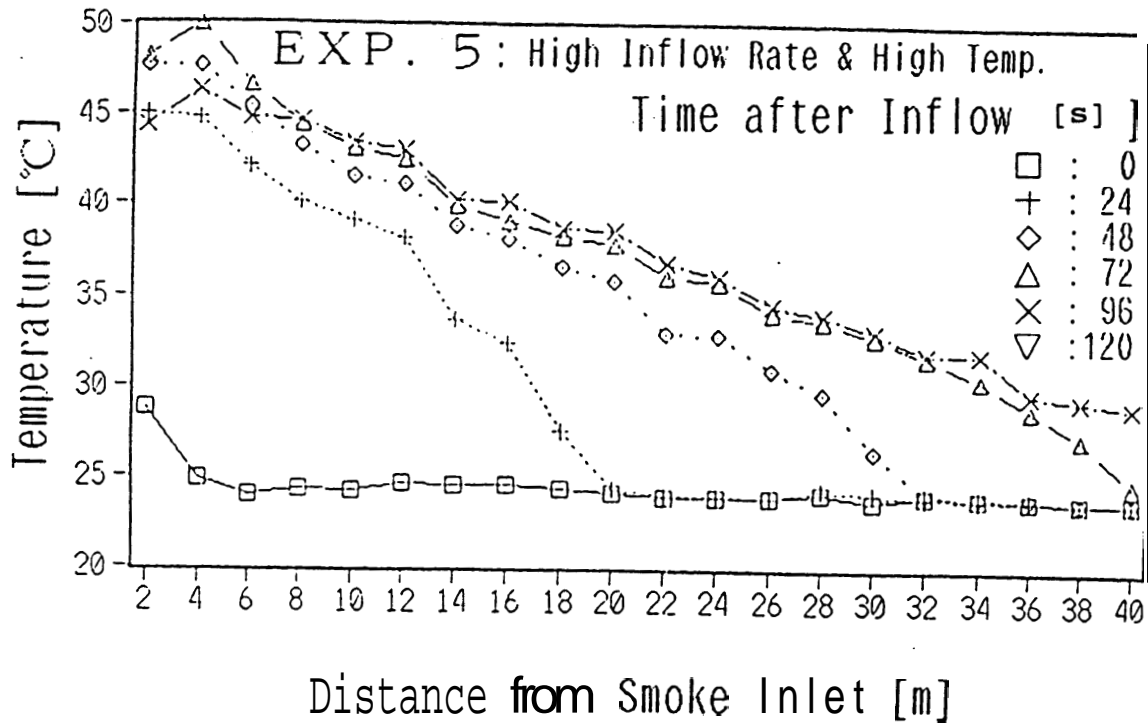


Figure 6-e

Distribution of Horizontal Maximum Temperature (Exp. 5-a)

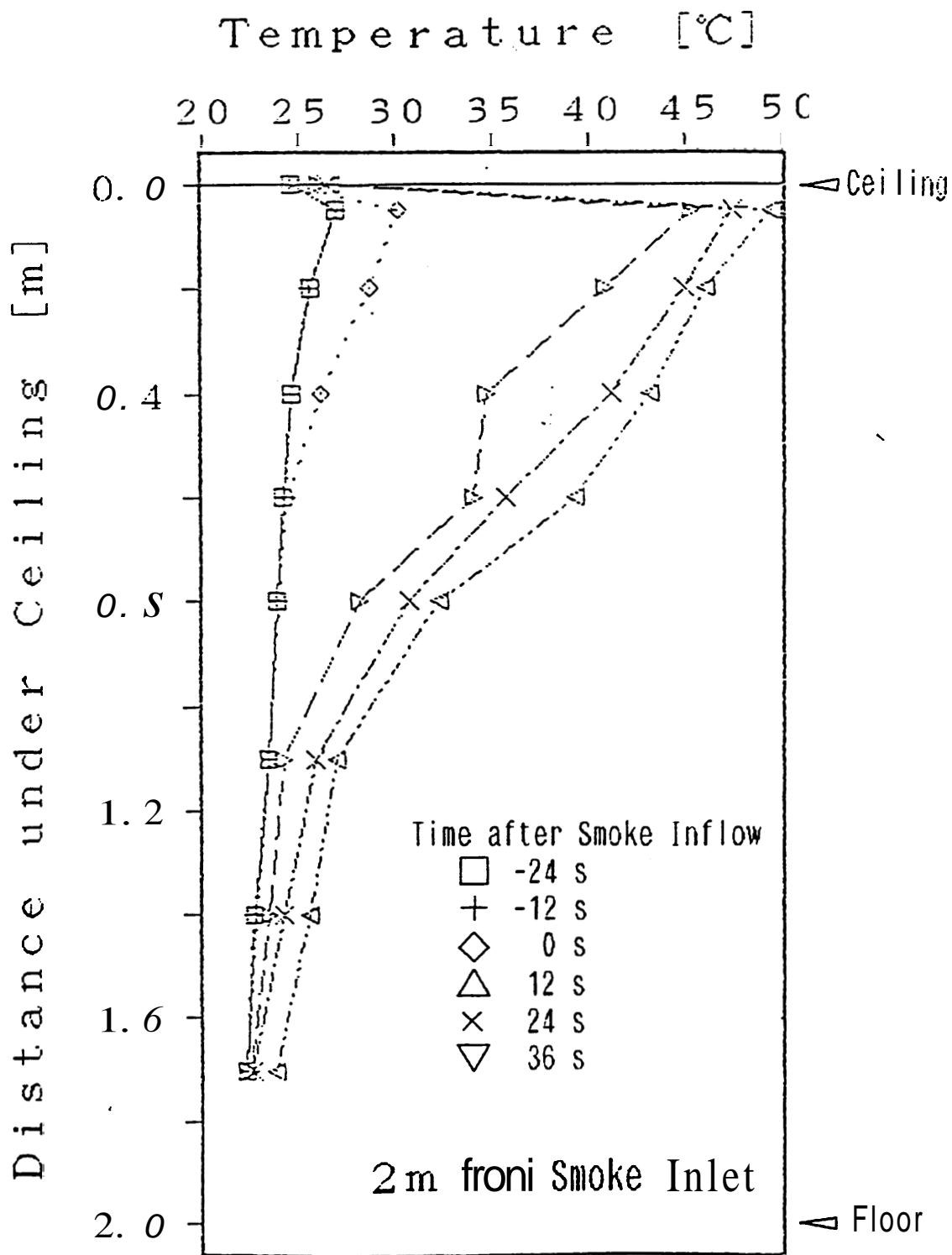


Figure 7-a Vertical Temperature Distribution at 2[m] (Exp.5)

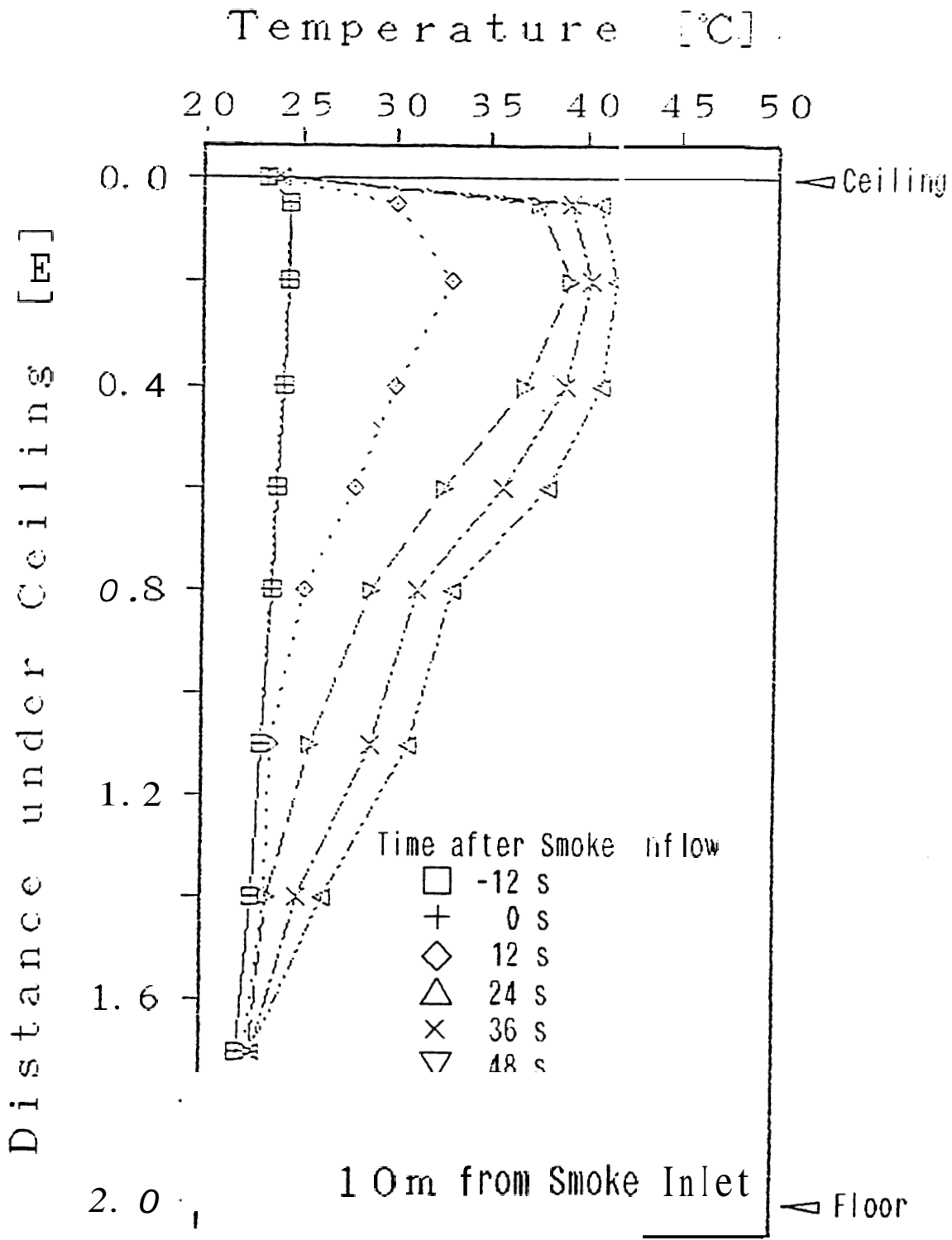


Figure 7-b Vertical Temperature Distribution at 10[m] (Exp.5)

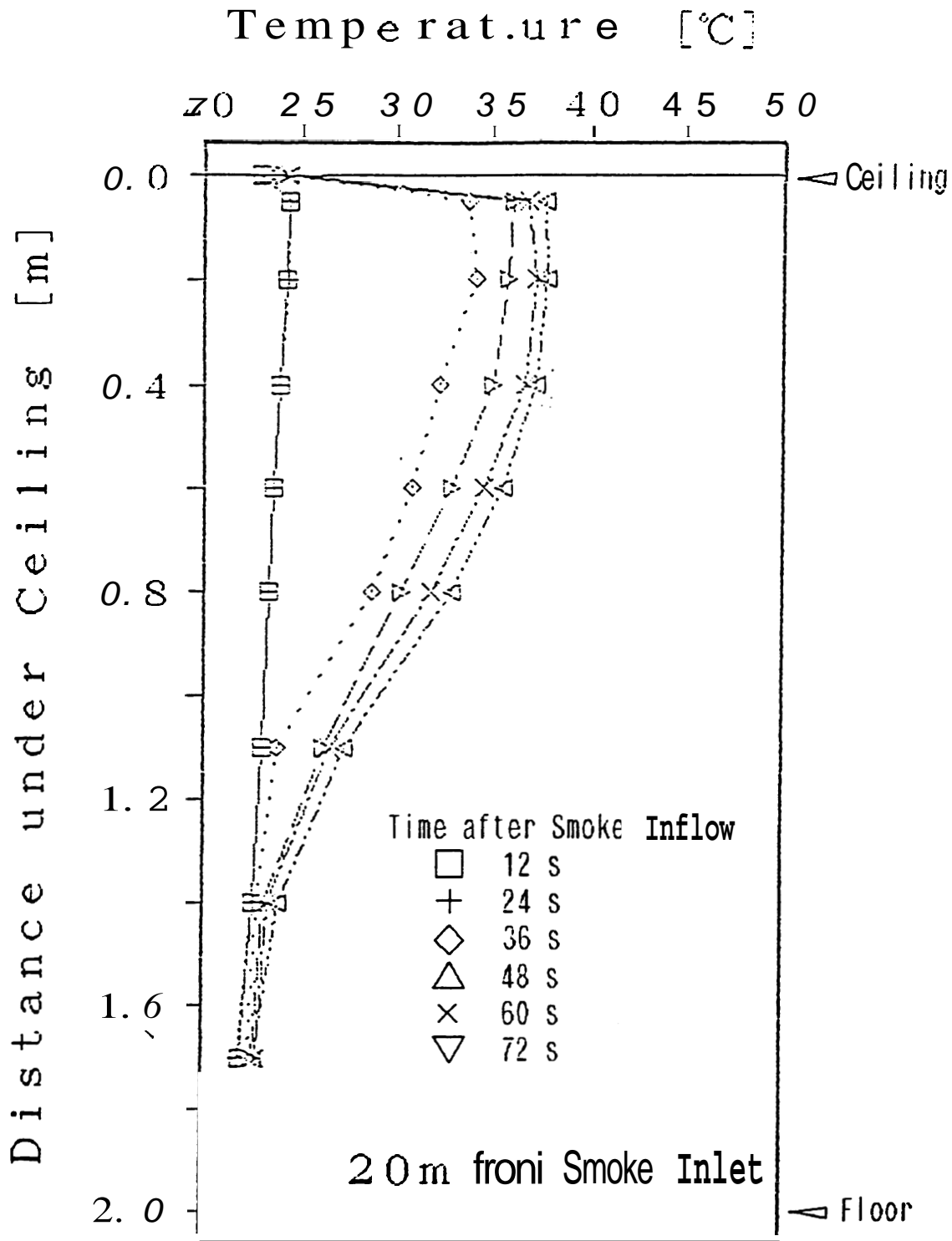


Figure 7-c Vertical Temperature Distribution at 20[m] (Exp.5)

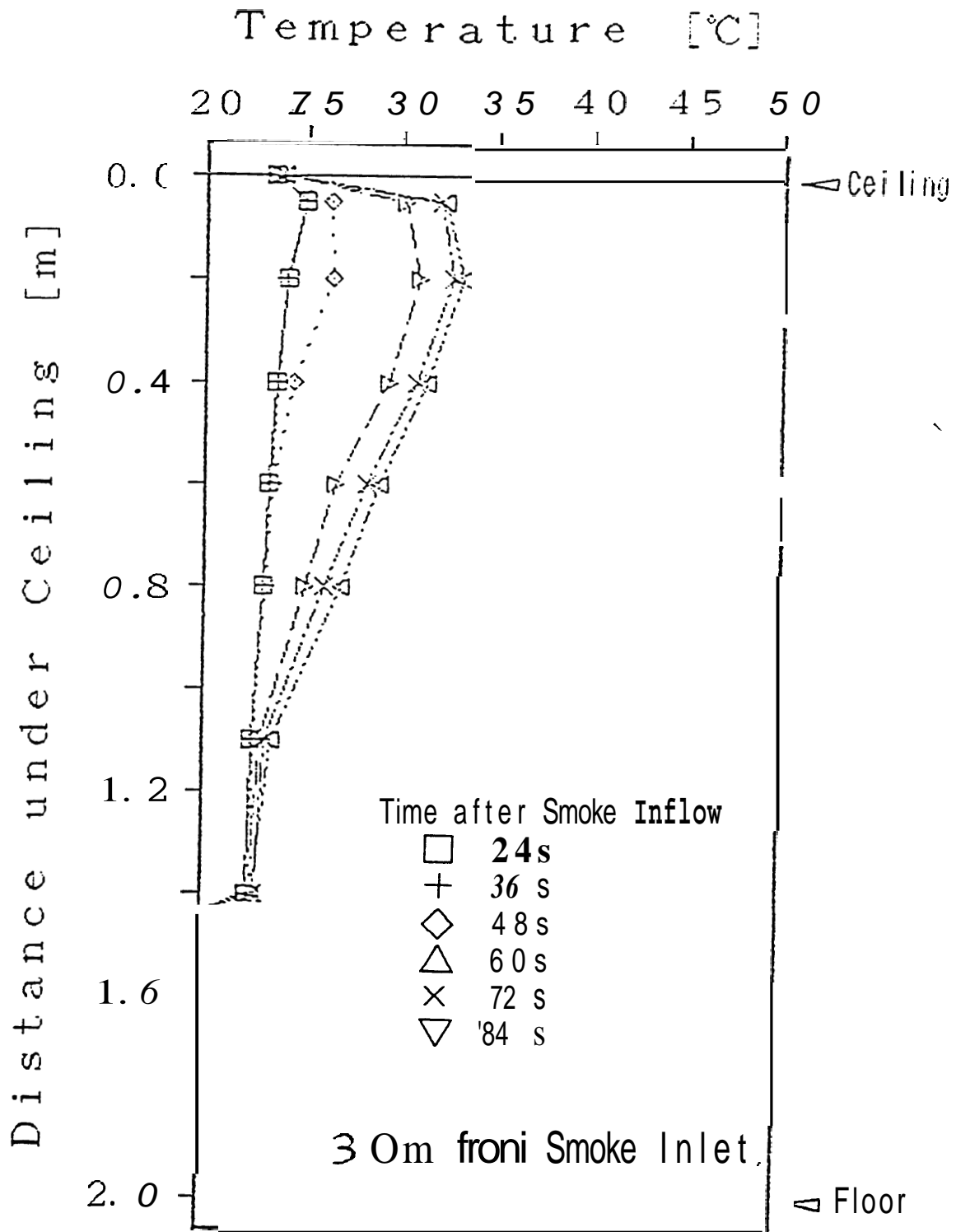


Figure 7-d Vertical Temperature Distribution at 30[m] (Exp.5)

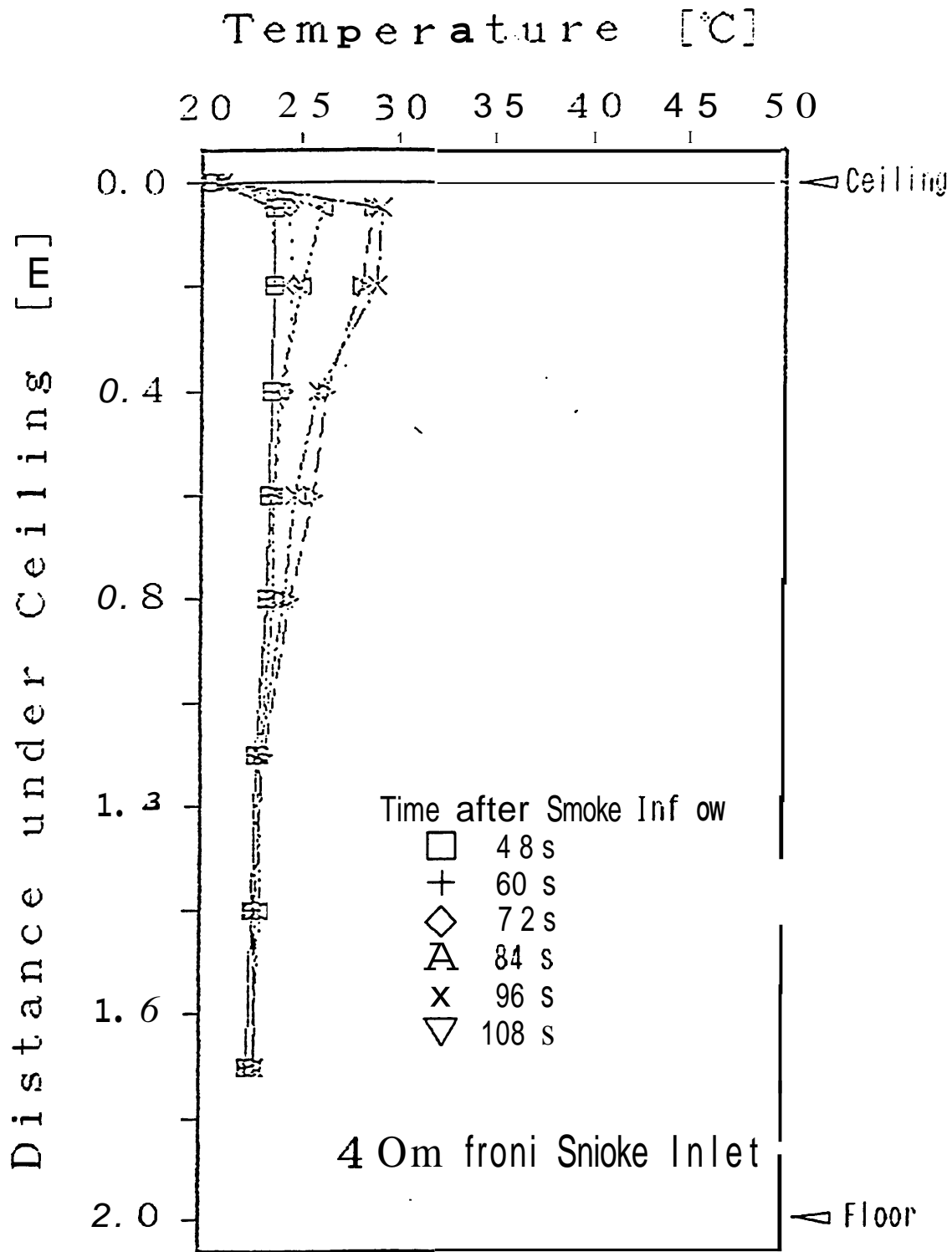
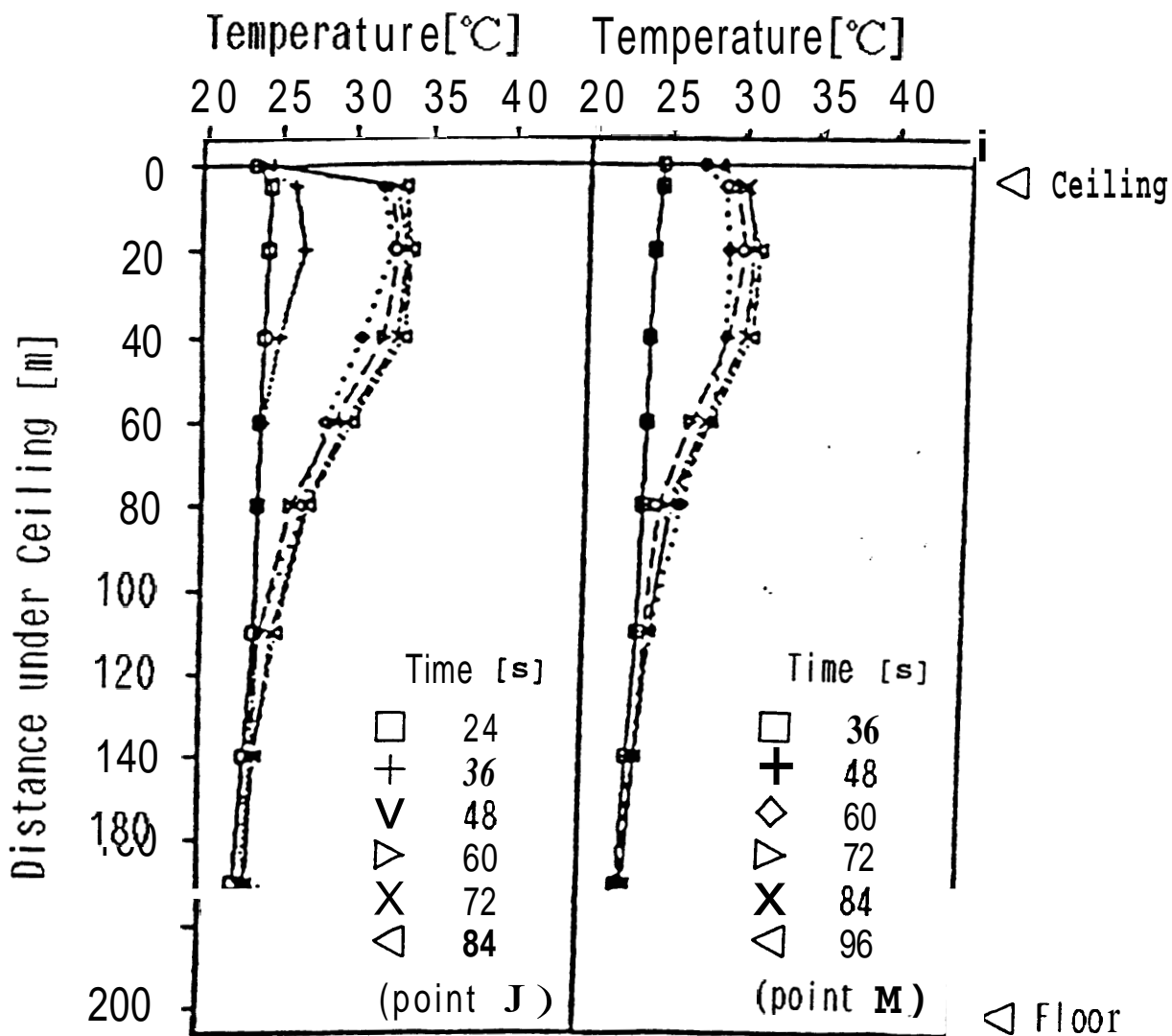


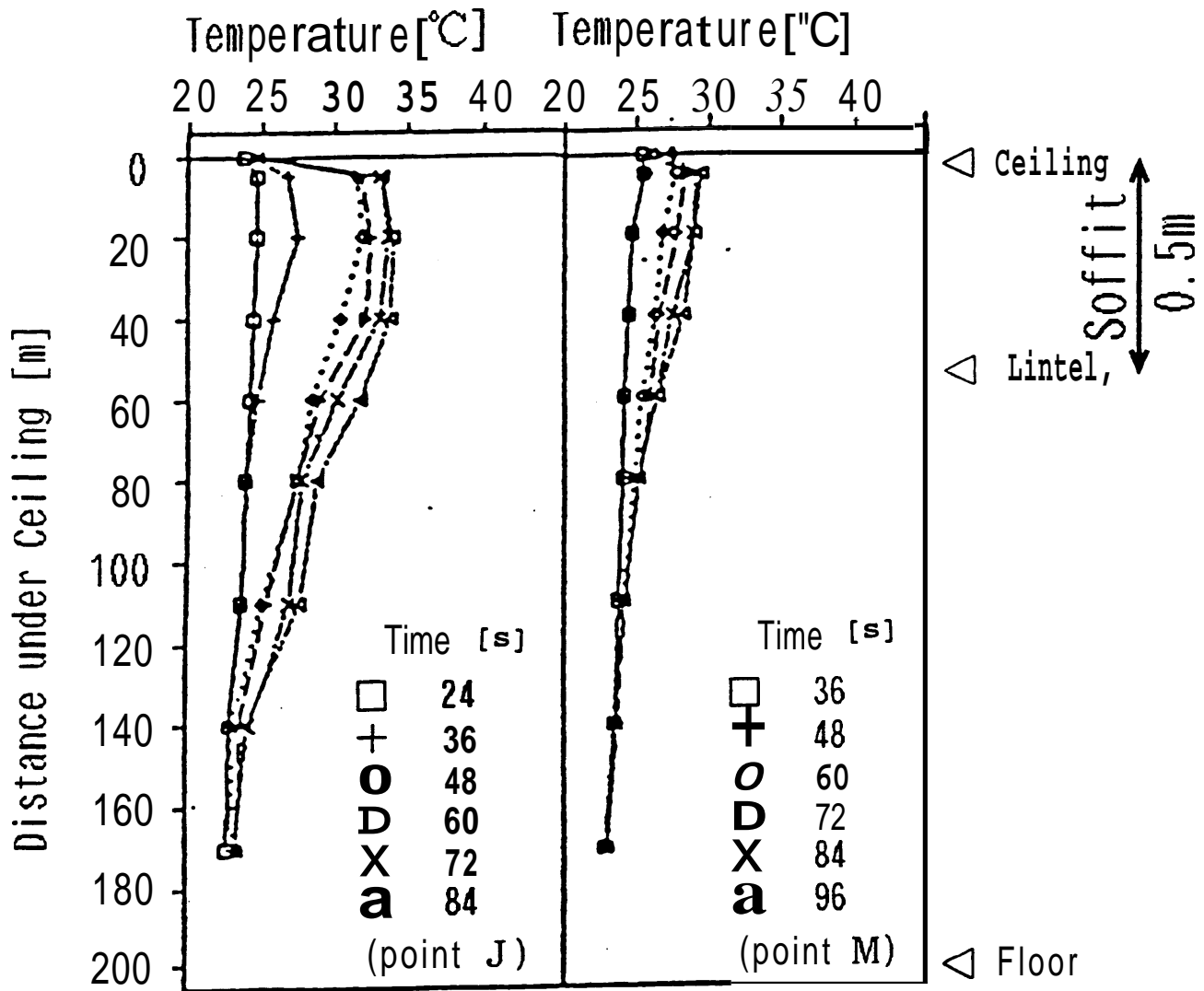
Figure 7-e Vertical Temperature Distribution at 40[m] (Exp.5)



20m from Inlet 26m from Inlet

Figure 8-a (Exp.2)

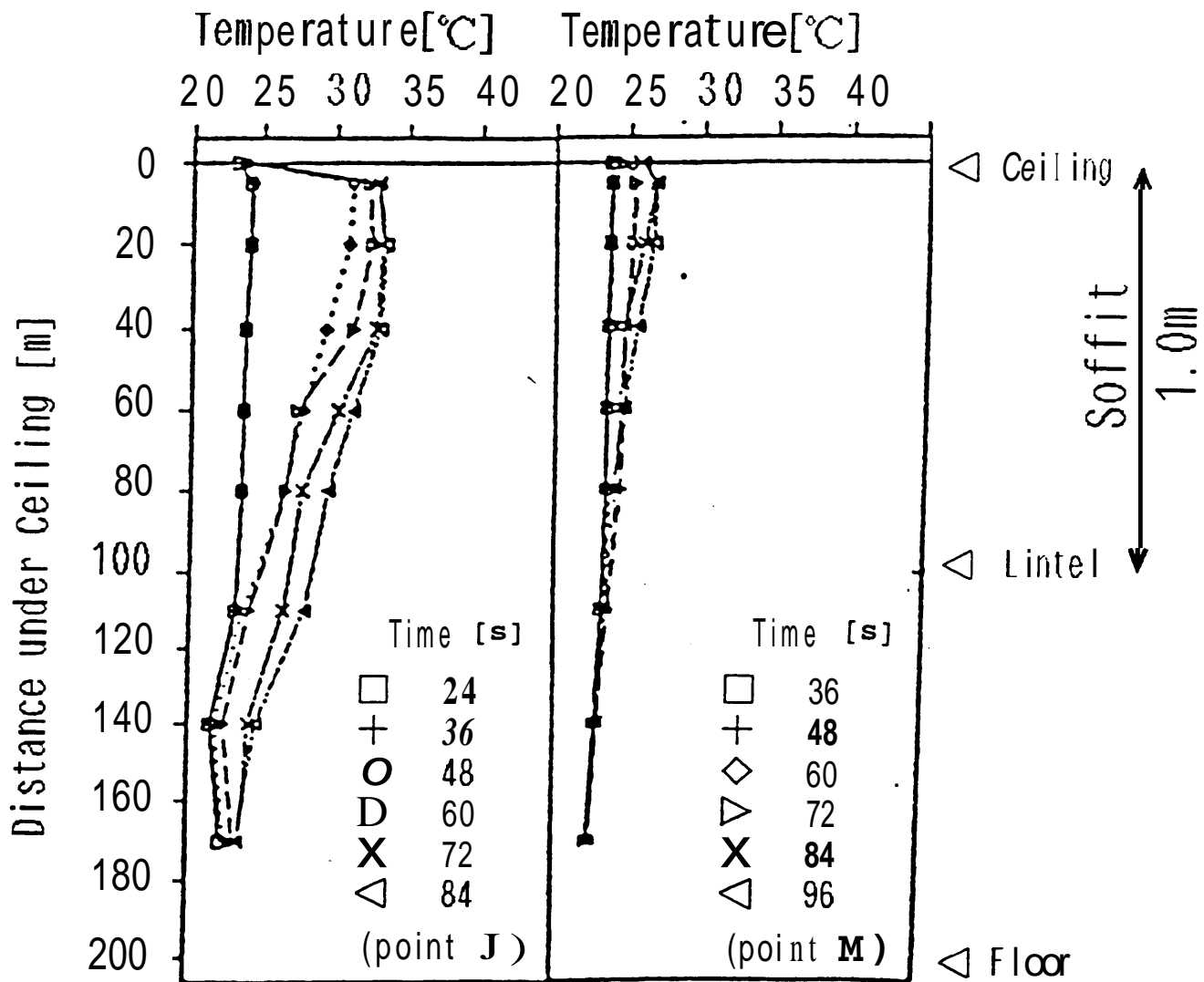
Vertical Distribution of Temperature
 In Case of 0.0m Soffit (23m from Inlet) (Exp.2-a)



20m from Inlet 26m from Inlet

Figure 8-b (Exp.2)

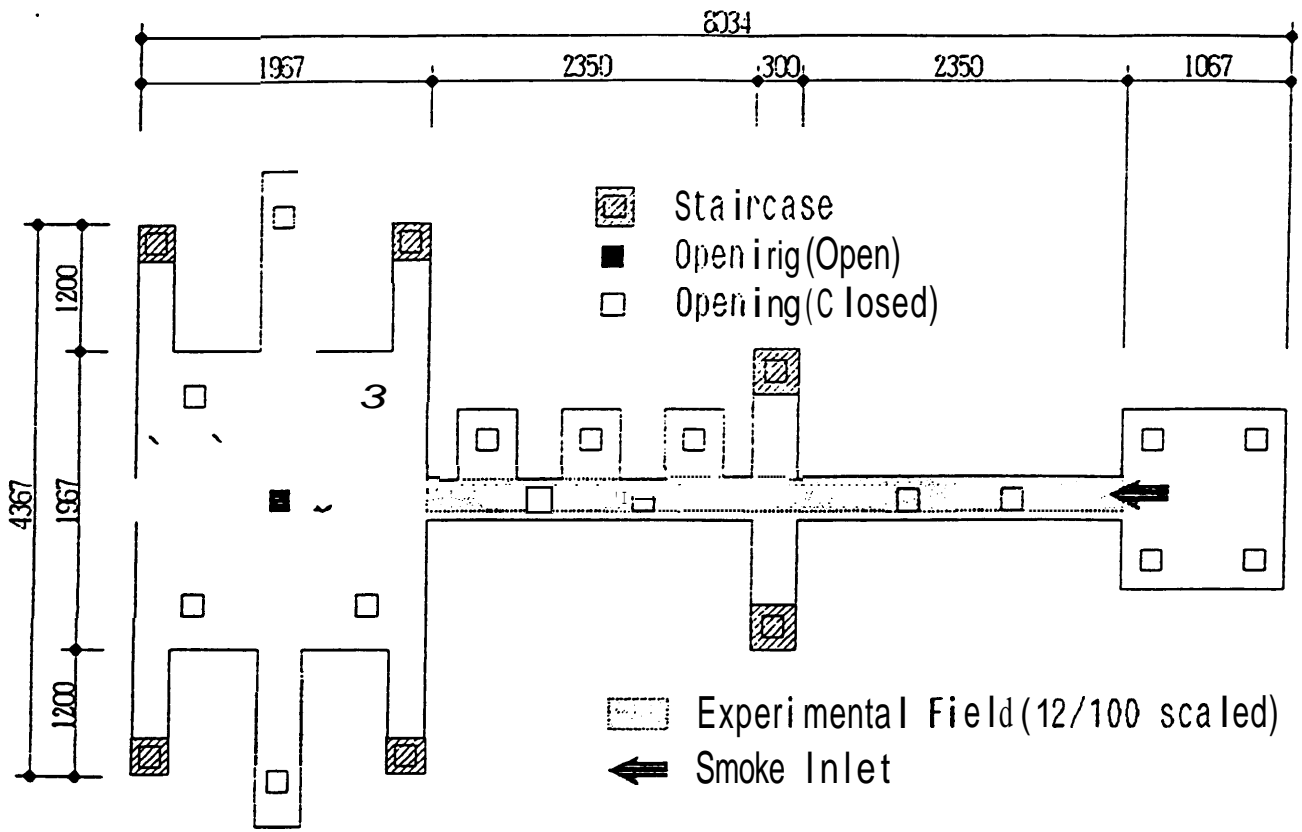
Vertical Distribution of Temperature In Case of 0.5m Soffit (23m from Inlet) (Exp.2-b)



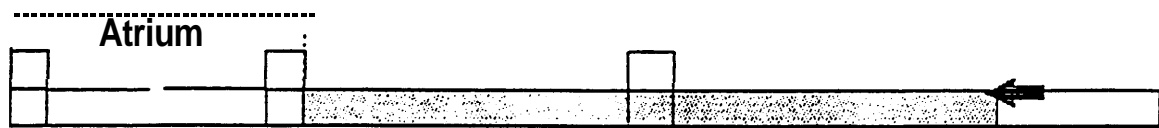
20m from Inlet 26m from Inlet

Figure 8-c (Exp.2)

Vertical Distribution of Temperature
 In Case of 1.0m Soffit (23m from Inlet) (Exp.2-c)



Plan of 1/20 Scaled Model of Underground Town



Section of 1/20 Scaled Model of Underground Town

Figure 9 A Corridor of Reduced Scale Model

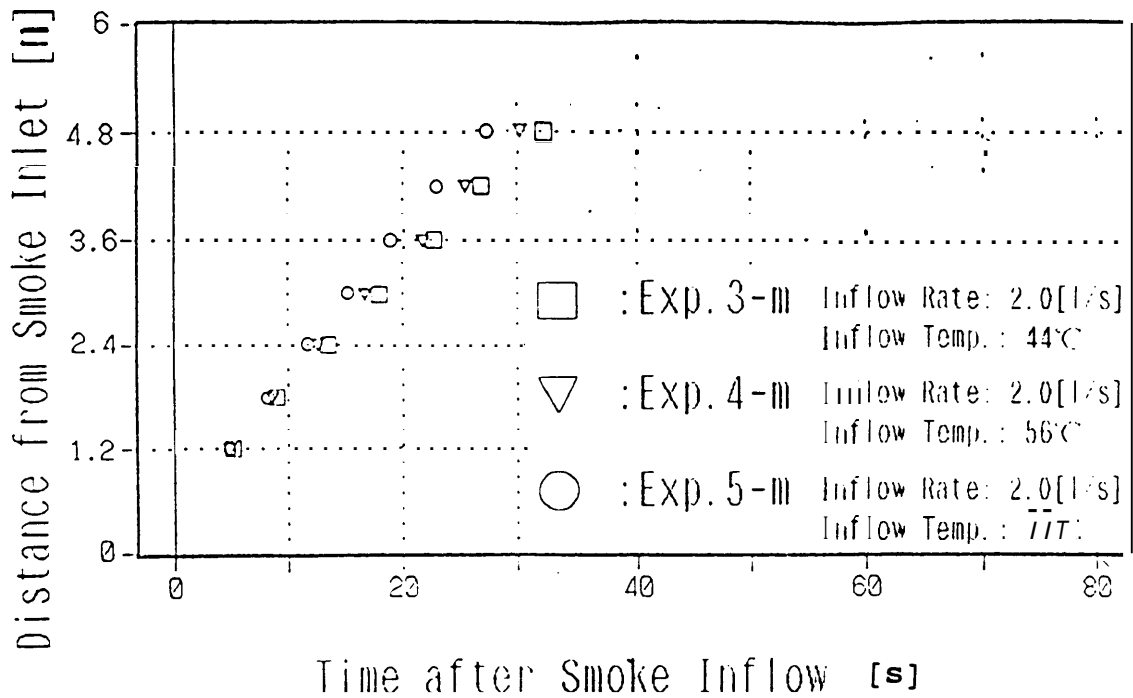


Figure 10 Location of Smoke Front Nose
(12/100 Scale)

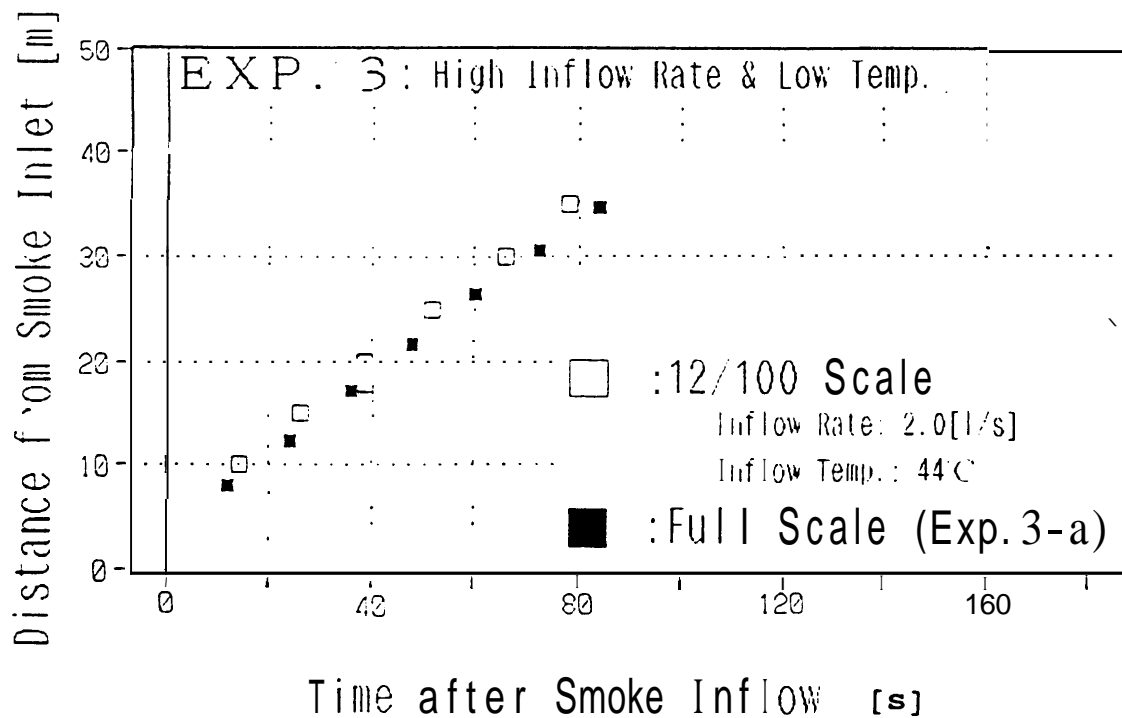


Figure 11-a Location of Smoke Front Nose
Comparison between Full Scale and 12/100 Scale (Exp. 3)

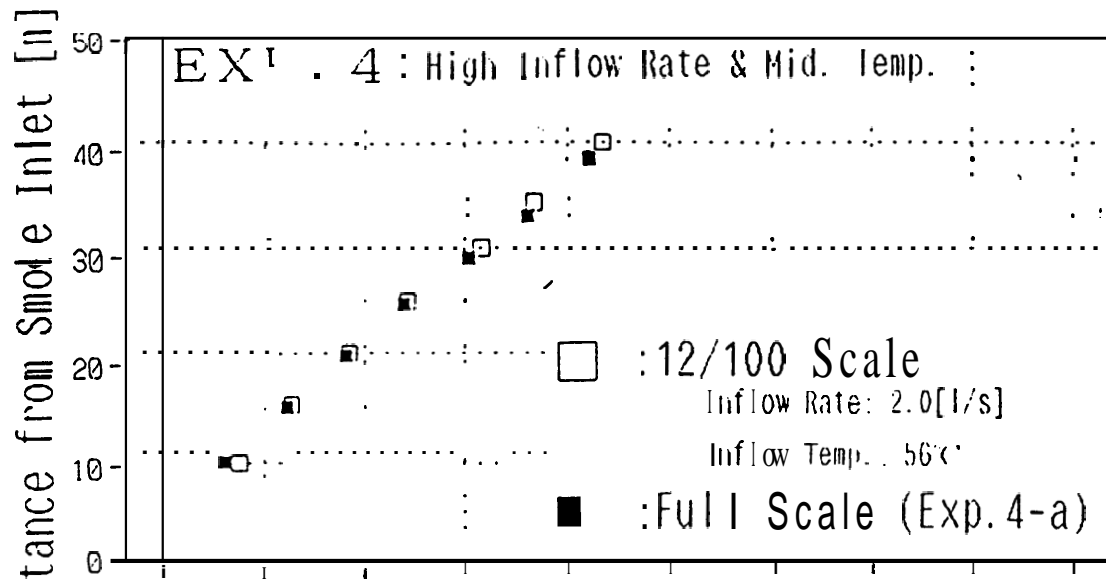


Figure 11-b Location of Smoke Front Nose
Comparison between full Scale and 12/100 Scale (Exp. 4)

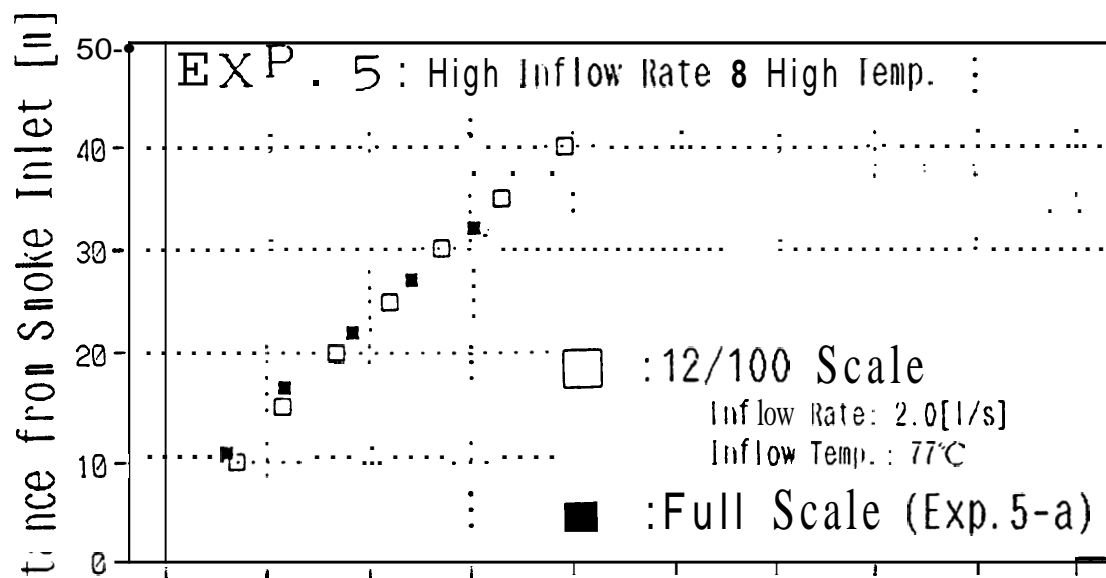


Figure 11-c Location of Smoke Front Nose
Comparison between full Scale and 12/100 Scale (Exp. 5)

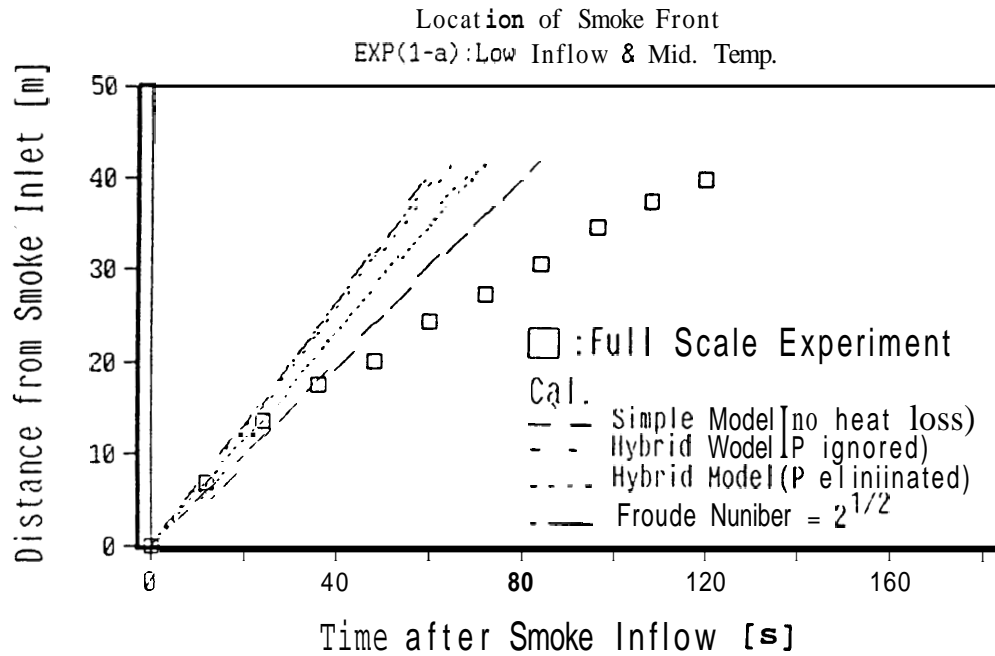


Figure 12-a Location of Smoke Front Nose
Comparison between Experiment and Calculation (Exp. 1-a)

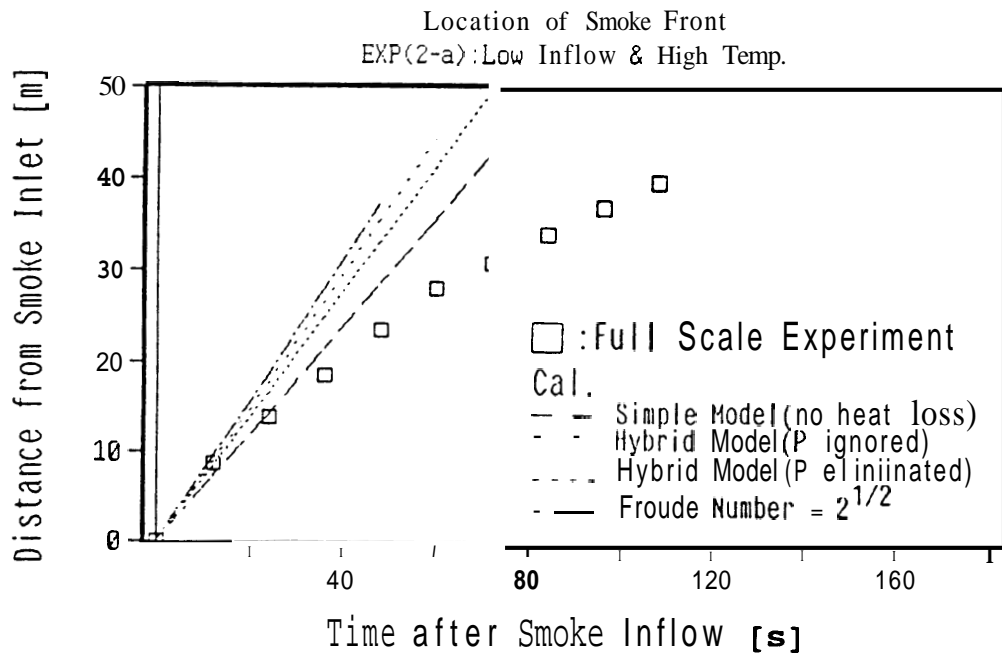


Figure 12-b Location of Smoke Front Nose
Comparison between Experiment and Calculation (Exp. 2-a)

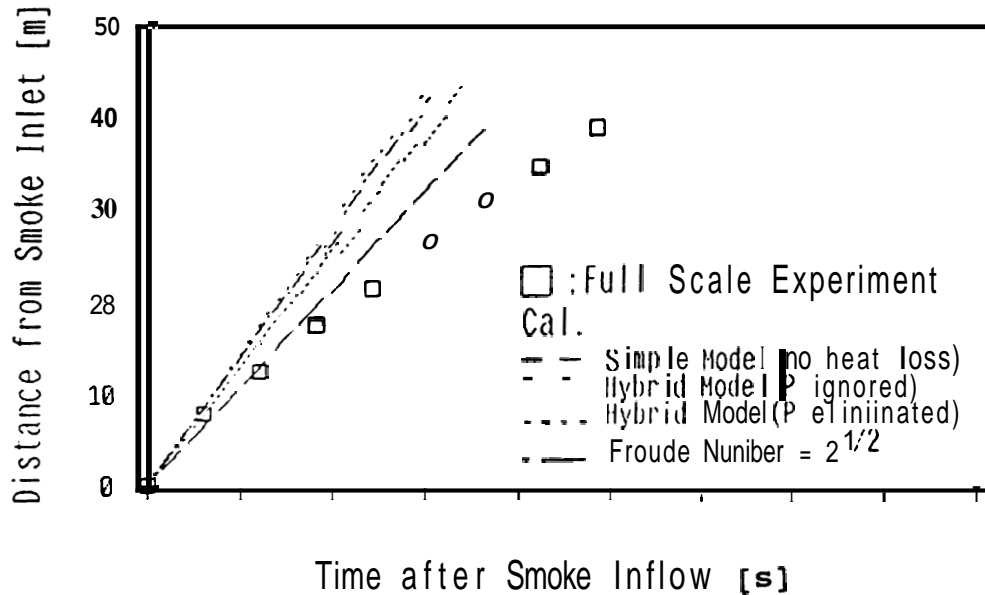


Figure 12-c

Location of Smoke Front Nose

Comparison between Experiment and Calculation (Exp. 3-a)

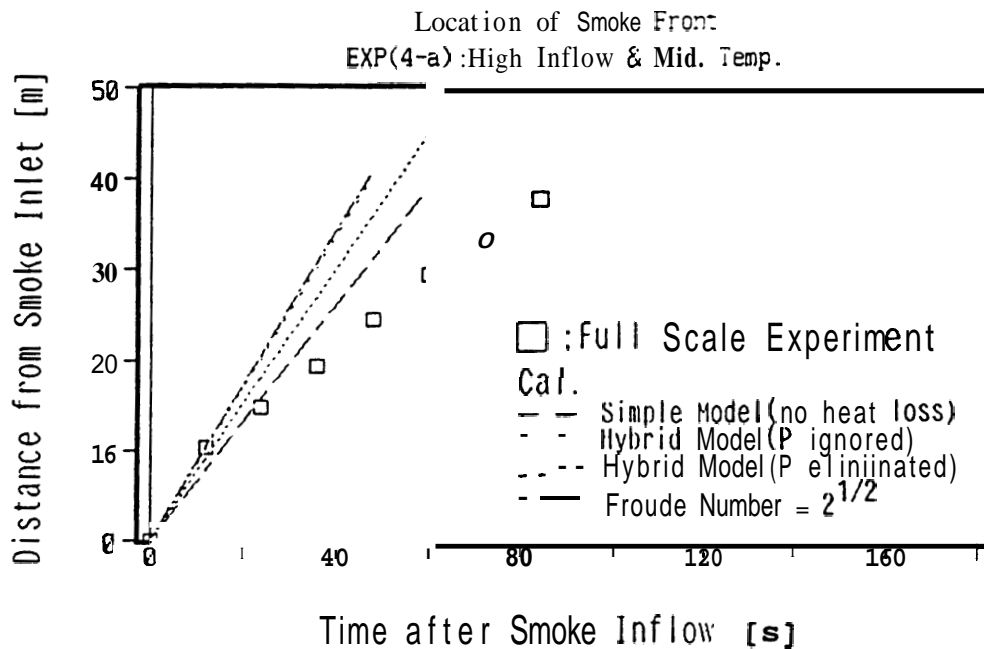


Figure 12-d

Location of Smoke Front Nose

Comparison between Experiment and Calculation (Exp. 4-a)

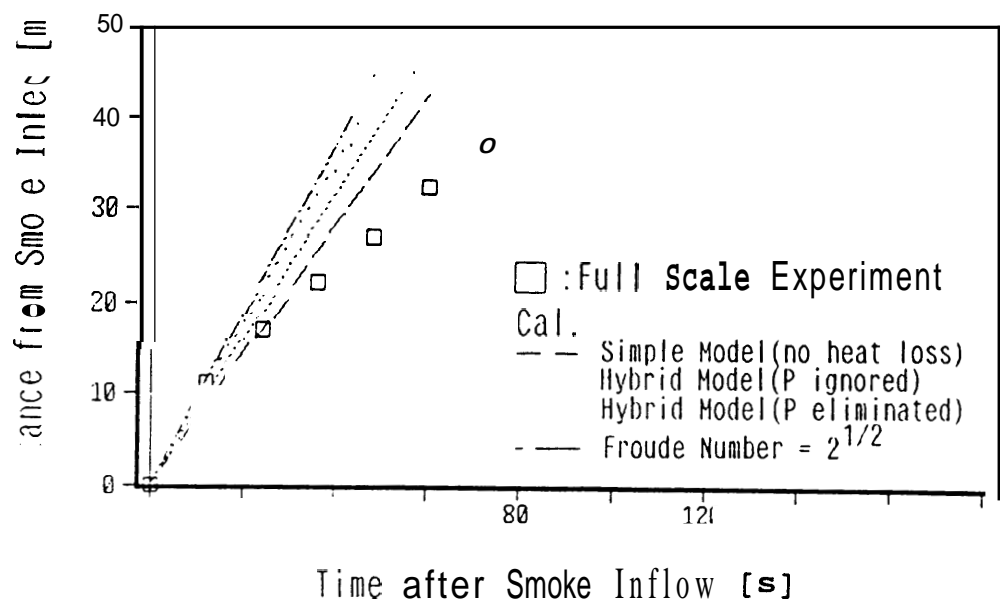
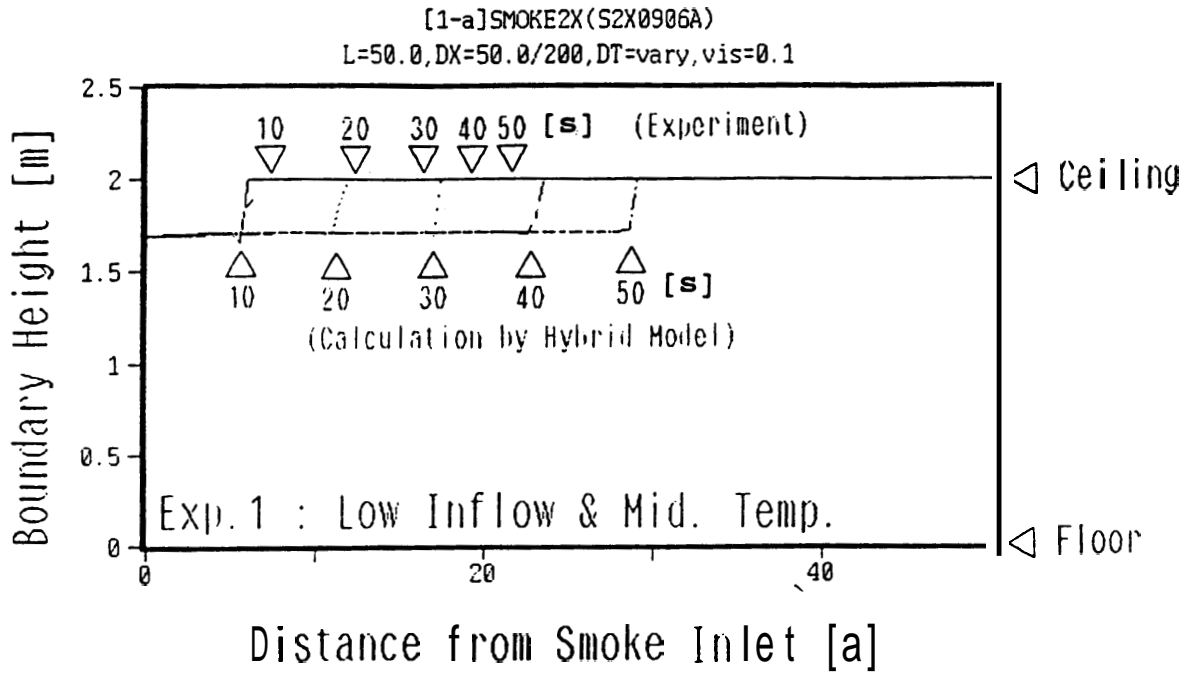


Figure 12-e

Location of Smoke Front Nose

Comparison between Experiment and Calculation (Exp. 5-a)



Comparison between Experiment and Calculation
for Location of Front(Nose) after Smoke Inflow

Figure 13-a (Exp.1-a) : Eliminated Case

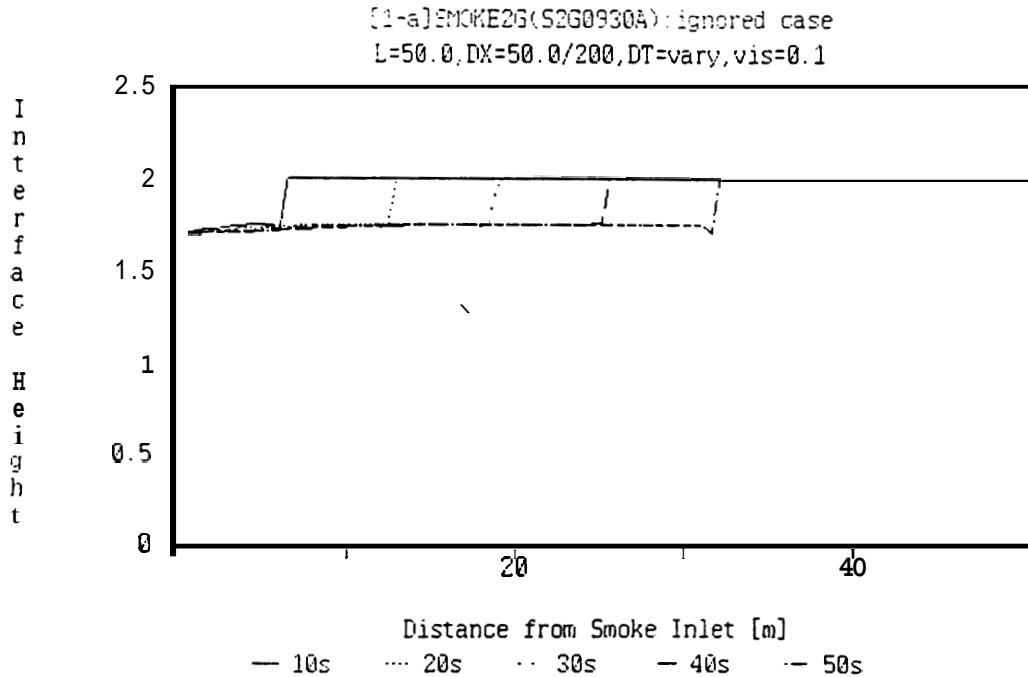
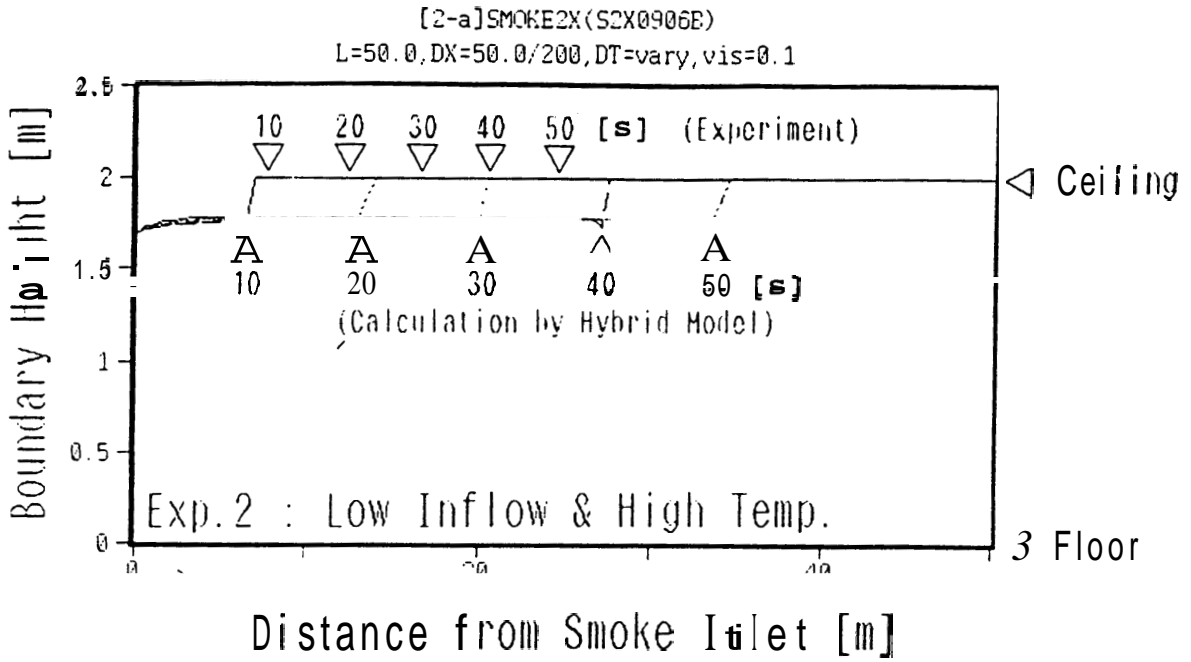


Figure 13-b Location of Smoke Front (Exp.1-a) : Ignored Case



Comparison between Experiment and Calculation for Location of Front(Nose) after Smoke Inflow

Figure 14-a (Exp.2-a) : Eliminated Case

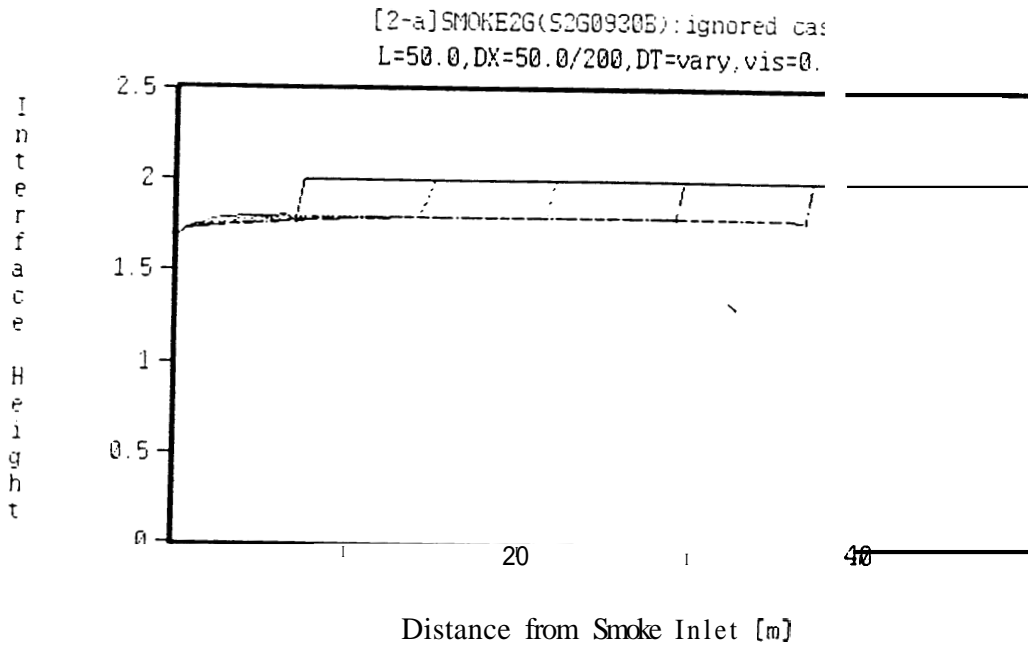
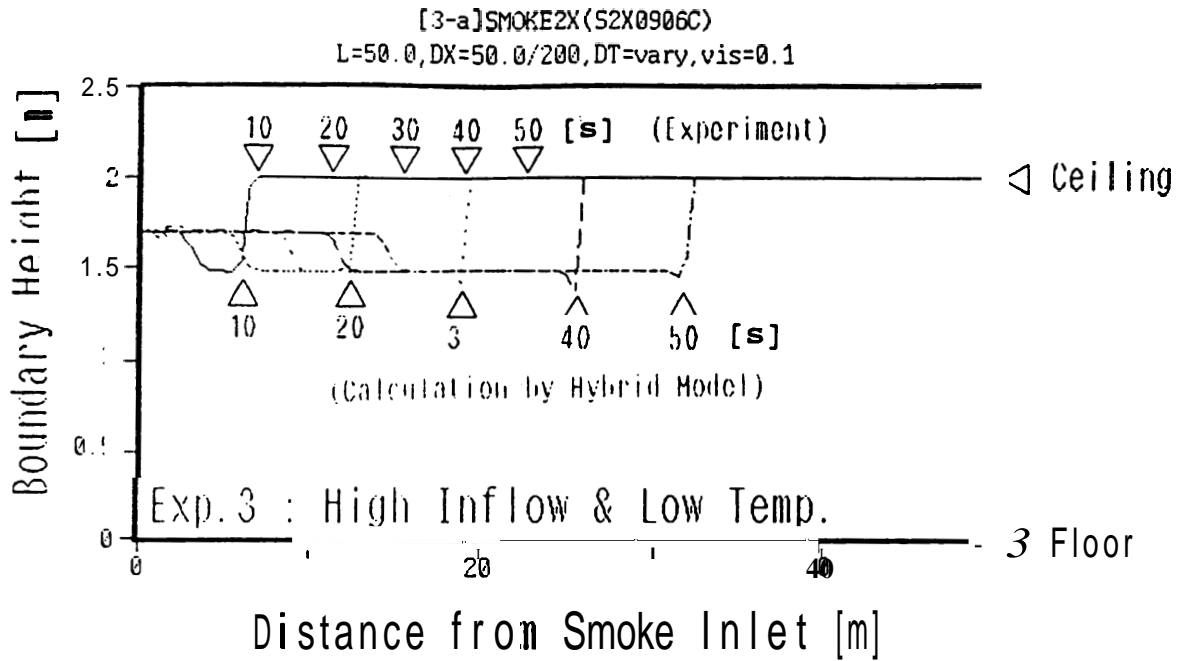


Figure 14-b Location of Smoke Front (Exp.2-a) : Ignored Case



Comparison between Experiment and Calculation
for Location of Front(Nose) after Smoke Inflow

Figure 15-a (Exp.3-a) : Eliminated Case

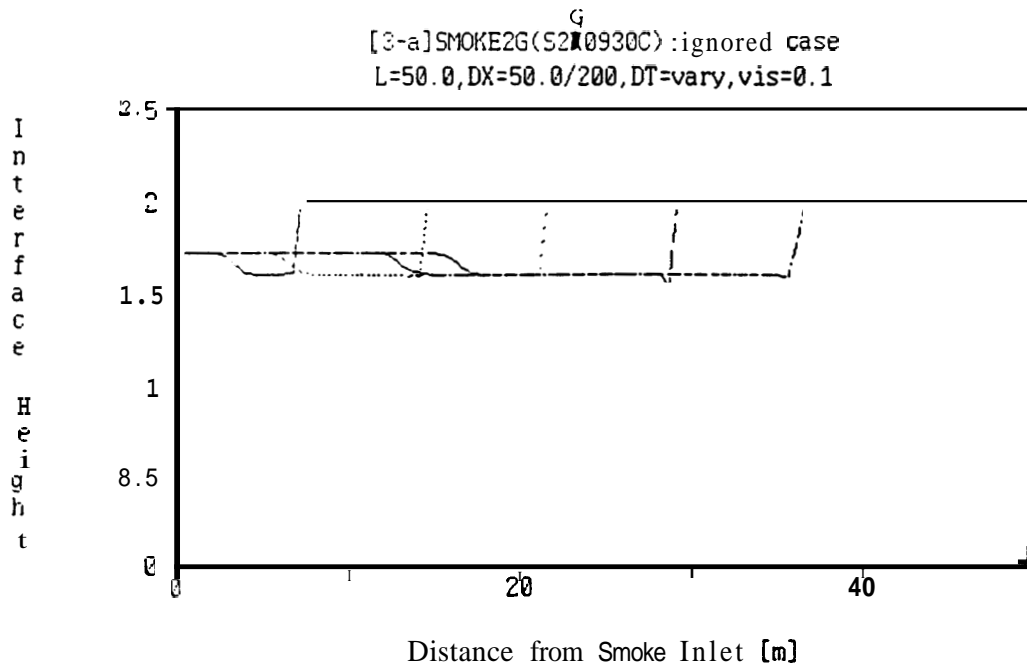
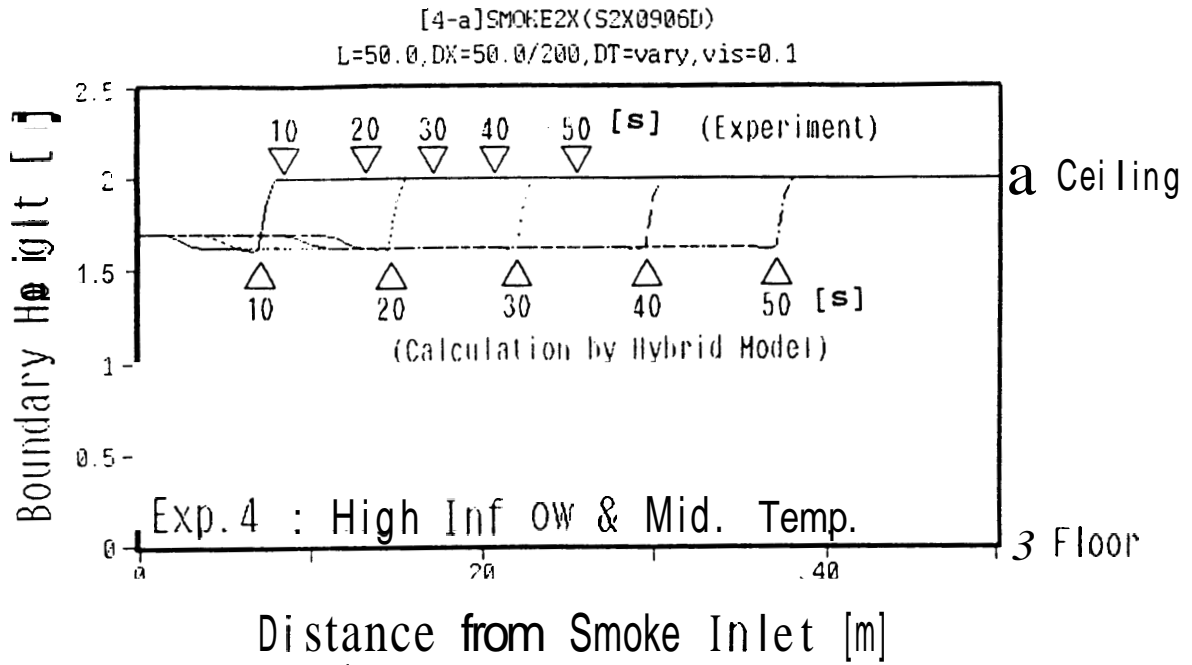


Figure 15-b Location of Smoke Front (Exp.3-a) : Ignored Case



Comparison between Experiment and Calculation
for Location of Front(Nose) after Smoke Inflow

Figure 16-a (Exp.4-a) : Eliminated Case

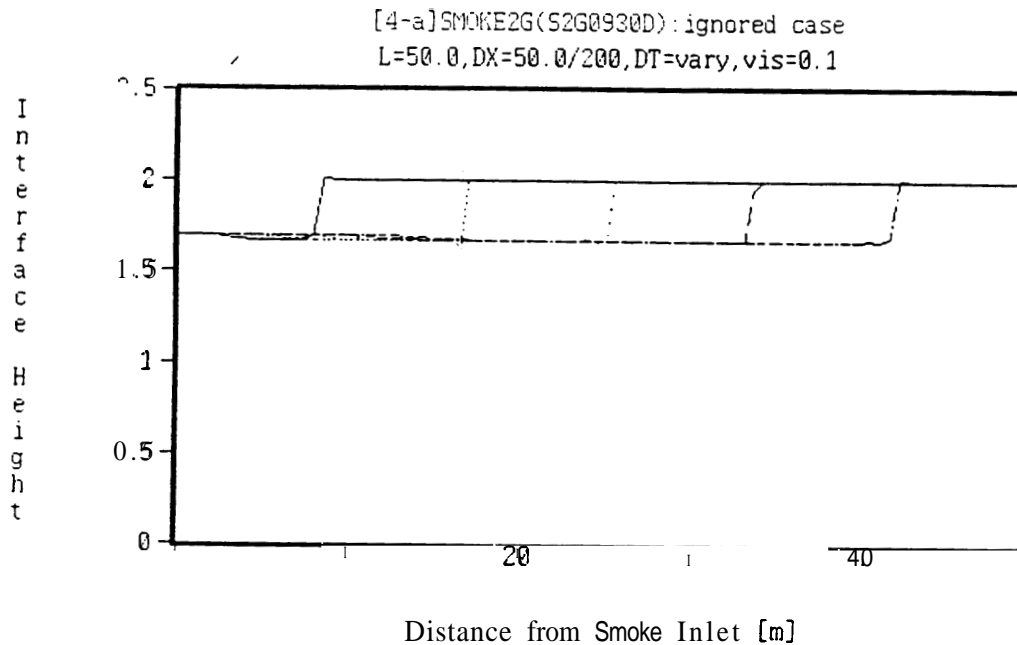
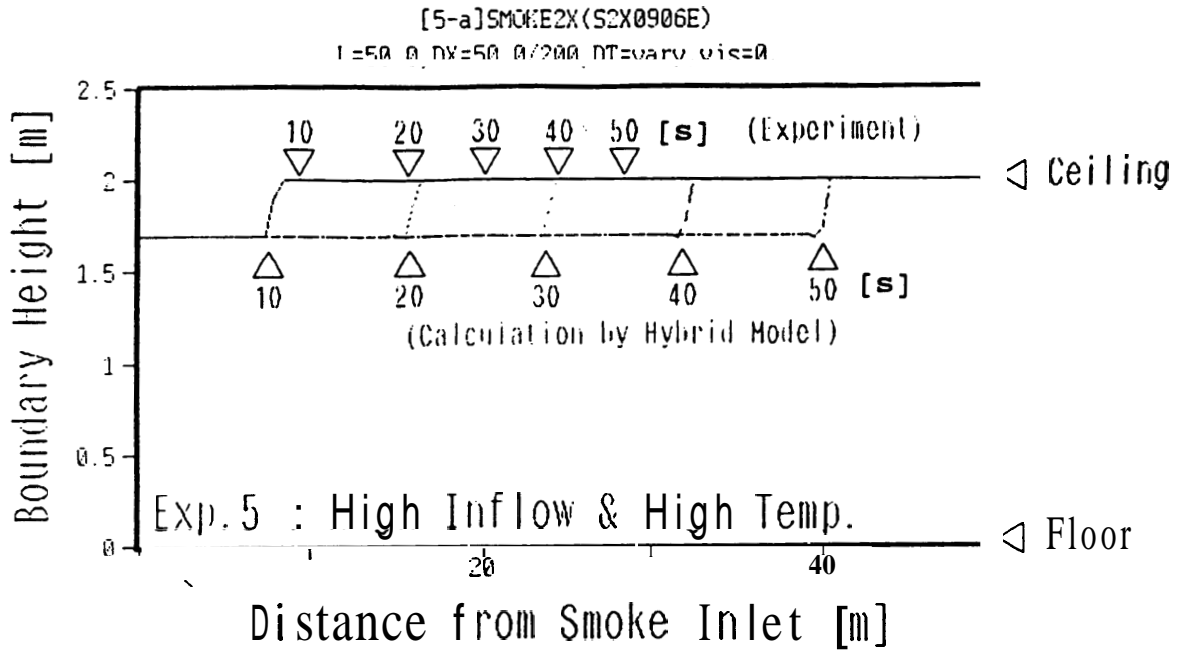


Figure 16-b Location of Smoke Front (Exp.4-a) : Ignored Case



Comparison between Experiment and Calculation
 for Location of Front(Nose) after Sniok Inflow

Figure 17-a (Exp.5-a) : Eliminated Case

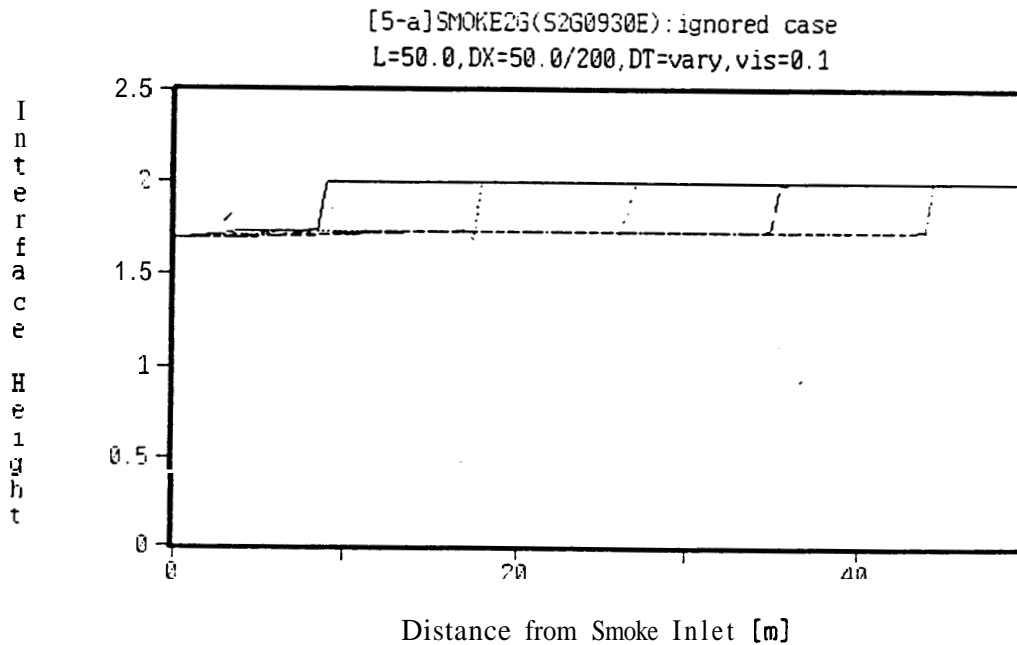


Figure 17-b Location of Smoke Front (Exp.5-a) : Ignored Case

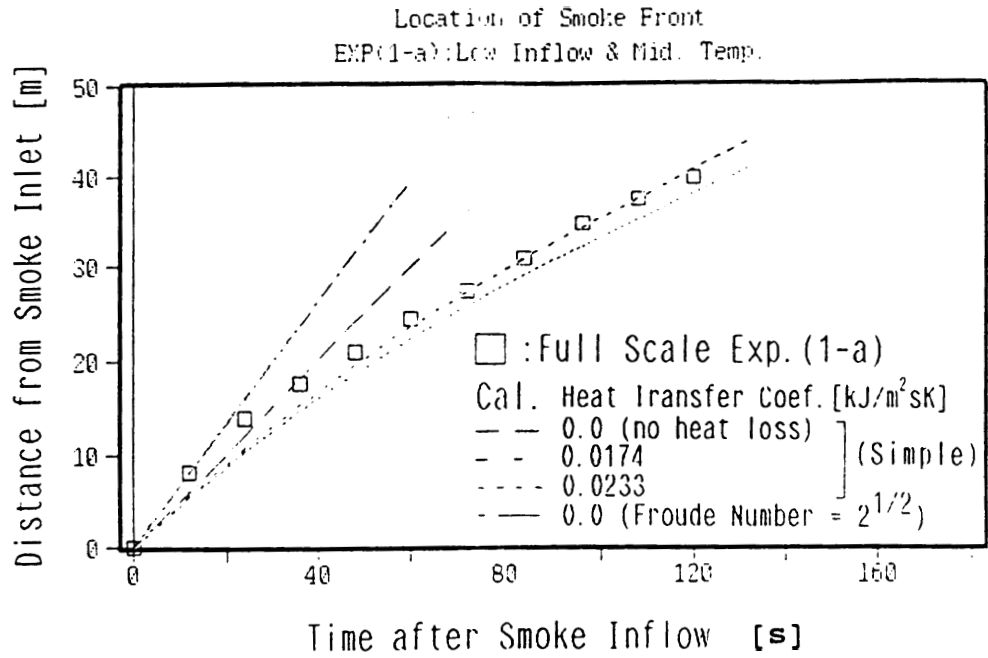


Figure 18-a (Exp.1-a) **Location of Smoke Front Nose**
Comparison between Experiment and Calculation

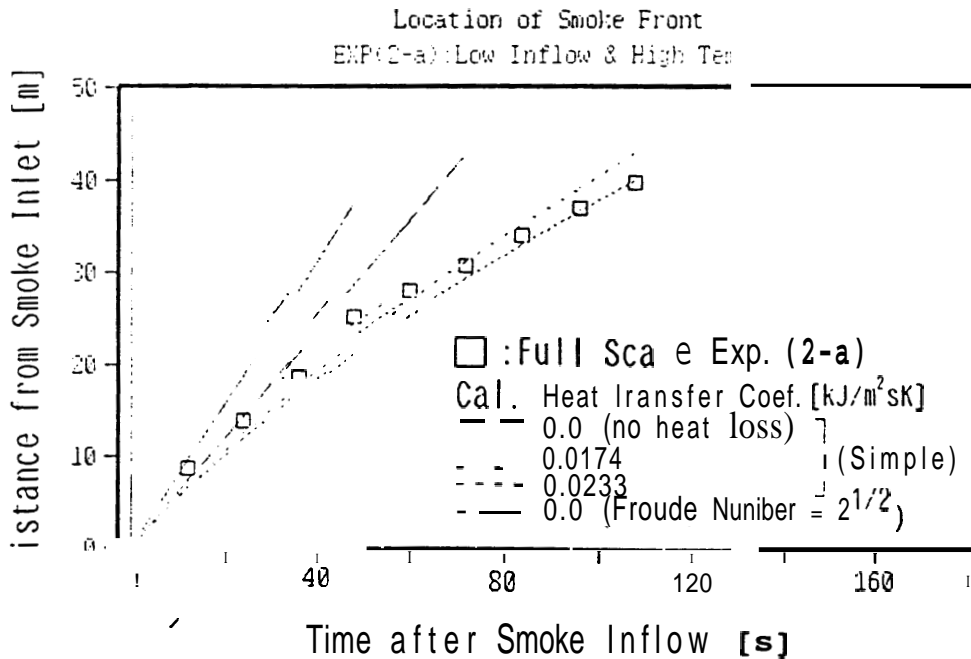


Figure 18-b (Exp.2-a) **Location of Smoke Front Nose**
Comparison between Experiment and Calculation

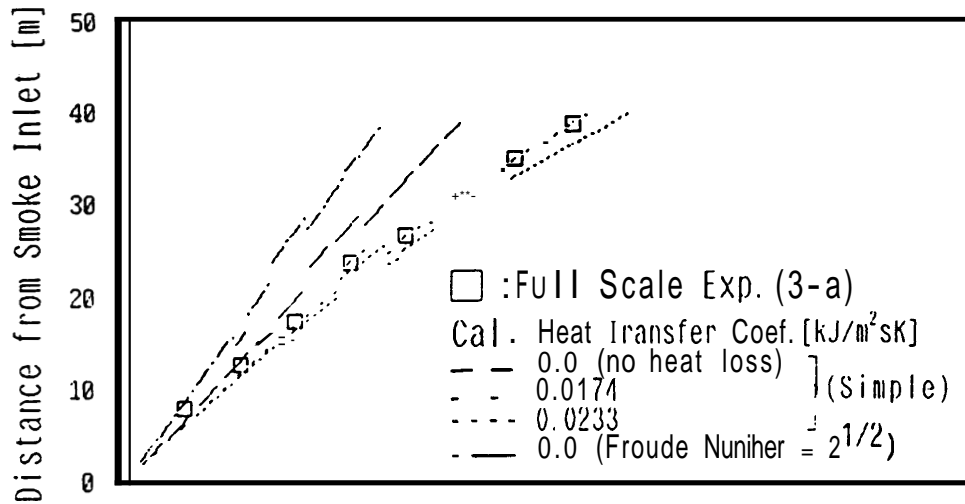


Figure 18-c (Exp.3-a) **Location of Smoke Front Nose**
Comparison between Experiment and Calculation

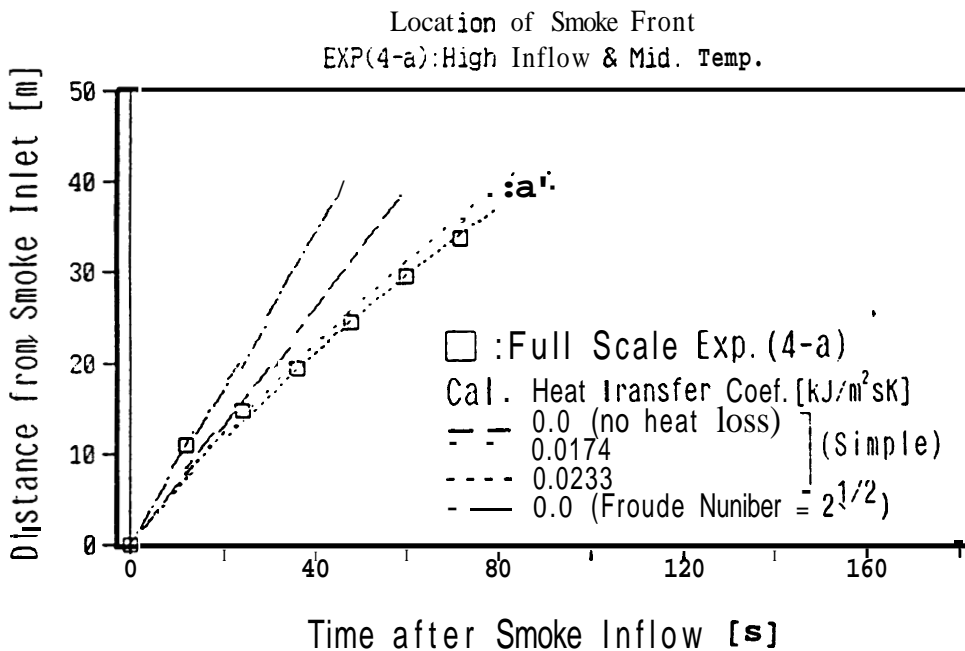


Figure 18-d (Exp.4-a) **Location of Smoke Front Nose**
Comparison between Experiment and Calculation

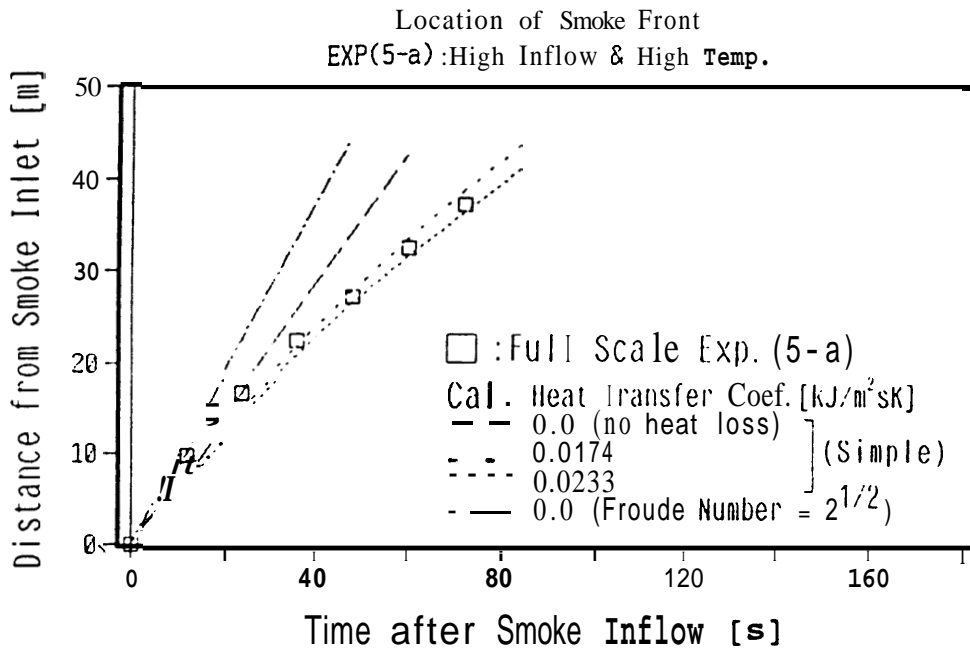


Figure 18-e (Exp.5-a)

Location of Smoke Front Nose
Comparison between Experiment and Calculation



| | | | | | |
|--|--|---|--|---|--|
| NIST-114A (REV. 3-90) | | U.S. DEPARTMENT OF COMMERCE NATIONAL INSTITUTE OF STANDARDS AND TECHNOLOGY | | 1. PUBLICATION OR REPORT NUMBER NTSTR 1987 | |
| BIBLIOGRAPHIC DATA SHEET | | | | 2. PERFORMING ORGANIZATION REPORT NUMBER | |
| | | | | 3. PUBLICATION DATE DECEMBER 1992 | |
| 1. TITLE AND SUBTITLE Smoke Movement in a Corridor - Hybrid Model, Simple Model and Comparison with Experiments | | | | | |
| 5. AUTHOR(S) Takayuki Matsushita and John H. Klote | | | | | |
| 6. PERFORMING ORGANIZATION (IF JOINT OR OTHER THAN NIST, SEE INSTRUCTIONS) U.S. DEPARTMENT OF COMMERCE NATIONAL INSTITUTE OF STANDARDS AND TECHNOLOGY GAITHERSBURG, MD 20899 | | | | 7. CONTRACT/GRANT NUMBER | |
| 8. TYPE OF REPORT AND PERIOD COVERED | | | | | |
| 10. SUPPLEMENTARY NOTES | | | | | |
| 11. ABSTRACT (A 200-WORD OR LESS FACTUAL SUMMARY OF MOST SIGNIFICANT INFORMATION. IF DOCUMENT INCLUDES A SIGNIFICANT BIBLIOGRAPHY OR LITERATURE SURVEY, MENTION IT HERE) | | | | | |
| <p>A hybrid model for modeling smoke movement in a corridor is described. This model uses a new approach for determining the corridor smoke flow. The hybrid model is a two zone model which considers velocities in each zone, and uses a fine mesh to the direction of propagation.</p> <p>Full scale and reduced scale experiments are described and compared with the results of the hybrid model. Since heat transfer is not presently considered, the velocity of spread is constant. But in the experiment, the velocity drops with advancing time.</p> <p>Two different approaches were used to deal with the pressure term, and it is not clear which approach is preferable.</p> <p>Finally, a simple model with heat transfer is described. This model is similar to the density flow model, and assumes the same effect of the opening flow in zone model for the front(nose) of smoke movement in a corridor. Results of the simple model are compared with the experiment with heat transfer, and the effect of the heat transfer coefficient is observed.</p> | | | | | |
| 12. KEY WORDS (6 TO 12 ENTRIES; ALPHABETICAL ORDER; CAPITALIZE ONLY PROPER NAMES; AND SEPARATE KEY WORDS BY SEMICOLONS) | | | | | |
| Comparison; corridor; heat transfer; hybrid model; large scale tests; reduced scale tests; smoke movement. | | | | | |
| 3. AVAILABILITY | | | | 14. NUMBER OF PRINTED PAGES | |
| <input checked="" type="checkbox"/> | UNLIMITED | | | 51 | |
| <input type="checkbox"/> | FOR OFFICIAL DISTRIBUTION. DO NOT RELEASE TO NATIONAL TECHNICAL INFORMATION SERVICE (NTIS). | | | 15. PRICE | |
| <input type="checkbox"/> | ORDER FROM SUPERINTENDENT OF DOCUMENTS, U.S. GOVERNMENT PRINTING OFFICE, WASHINGTON, DC 20402. | | | A04 | |
| <input checked="" type="checkbox"/> | ORDER FROM NATIONAL TECHNICAL INFORMATION SERVICE (NTIS), SPRINGFIELD, VA 22161. | | | | |

ELECTRONIC FORM

